JAN 1988 2

AD-A192 027 DTIC ELECTE MAR 08 1988 S D

REPORT DOCUMENTATION PAGE

1a. RESTRICTIVE MARKINGS	
2a. SECURITY CLASSIFICATION AUTHORITY	3. DISTRIBUTION/AVAILABILITY OF REPORT Approved for public release; distribution unlimited.
2b. DECLASSIFICATION/DOWNGRADING SCHEDULE	
4. PERFORMING ORGANIZATION REPORT NUMBER(S) MSL-AF-AR2	5. MONITORING ORGANIZATION REPORT NUMBER(S) AFOSR-TR. 88-0216
6a. NAME OF PERFORMING ORGANIZATION Dept of Mechanical Engineering University of Rhode Island	6b. OFFICE SYMBOL (If applicable) URI
7a. NAME OF MONITORING ORGANIZATION AFOSR/NA	
6c. ADDRESS (City, State and ZIP Code) Kingston, RI 02881	7b. ADDRESS (City, State and ZIP Code) Building 410 Bolling Air Force Base DC 20332-6448
8a. NAME OF FUNDING/SPONSORING ORGANIZATION AFOSR	8b. OFFICE SYMBOL (If applicable) NA
9. PROCUREMENT INSTRUMENT IDENTIFICATION NUMBER AFOSR-85-0362	
8c. ADDRESS (City, State and ZIP Code) Bolling Air Force Base DC 20332-6448 Bldg 410	10. SOURCE OF FUNDING NOS. PROGRAM ELEMENT NO: 61102F PROJECT NO: 2302 TASK NO: B2 WORK UNIT NO:
11. TITLE (Include Security Classification) Study of Probabilistic Fatique Crack Growth and Associated Scatter	
12. PERSONAL AUTHOR(S) Hamouda Ghonem Under Constant-And-Variable Amplitude Loading Spectrum	
13a. TYPE OF REPORT Annual	13b. TIME COVERED FROM 2/15/86 TO 2/15/87
14. DATE OF REPORT (Yr., Mo., Day) Sept. 6, 1987	15. PAGE COUNT 61
16. SUPPLEMENTARY NOTATION	

17. COSATI CODES		
FIELD	GROUP	SUB. GR.

18. SUBJECT TERMS (Continue on reverse if necessary and identify by block number)
Transition probability, Delay time, Stochastic

19. ABSTRACT (Continue on reverse if necessary and identify by block number)

The objective of the program's second year research work was to examine the validity of the constant probability crack growth model while refining the transition intensity parameter. This work has been completed, thus leading to a crack growth rate equation with an explicit probability term. Furthermore, work extending the applicability of the model to variable loading required the determination of the delay-time associated with a single overload. An experimental test program was carried out on a titanium alloy using a potential drop technique to record crack length increments as function of overload characteristics. This program has been completed and results will be incorporated into the basic stochastic model.

20. DISTRIBUTION/AVAILABILITY OF ABSTRACT	21. ABSTRACT SECURITY CLASSIFICATION
UNCLASSIFIED/UNLIMITED ☒ SAME AS RPT ☐ DTIC USERS ☐	Unclassified

22a. NAME OF RESPONSIBLE INDIVIDUAL	22b. TELEPHONE NUMBER (Include Area Code)	22c. OFFICE SYMBOL
Lt.Col. Major G. Haritos	(202)767-0463	~~AFOSR~~ NA

DD FORM 1473, 83 APR EDITION OF 1 JAN 73 IS OBSOLETE.

SECURITY CLASSIFICATION OF THIS PAGE

STUDY OF PROBABILISTIC FATIGUE CRACK GROWTH AND ASSOCIATED SCATTER UNDER CONSTANT-AND-VARIABLE AMPLITUDE LOADING SPECTRUM

Report on efforts in the period
15 July 1986 to 15 July 1987

Contract: Grant AFOSR-85-0382
Principal Investigator: Prof. H. Ghonem
Dept. of Mechanical Engineering
& Applied Mechanics
University of Rhode Island

Date: September 6, 1987

SUMMARY

The objective of the program's second year research work was to examine the validity of the constant probability crack growth model while refining the transition intensity parameter. This work has been completed, thus leading to a crack growth rate equation with an explicit probability term. Furthermore, work extending the applicability of the model to variable loading required the determination of the delay-time associated with a single overload. An experimental test program was carried out on a titanium alloy using a potential drop technique to record crack length increments as function of overload characteristics. This program has been completed and results will be incorporated into the basic stochastic model.

2. REPORT

Details of the research efforts and status of the research are described in the attached two papers. One was published by the J. Eng. Fracture Mechanics and the second has been accepted for publication.

3. PERSONNEL ASSOCIATED WITH THE RESEARCH EFFORTS

Mr. Peter Neilans
Research Engineer

Mr. V. Agrawal
degree: Master of Science

Mr. D. Zheng
degree: Ph.D.
expected date: July 1990

4. INTERACTIONS

1. A paper entitled "Constant-Probability Crack Growth Curves" was presented at the 20th National Symposium on Fracture Mechanics, Lehigh University, 23-25 June 1987.
2. An invitation was extended by Professor A. Pineau of Ecole des Mines to deliver a lecture on the stochastic crack growth modelling. The date of the seminar is October 14, 1987.

TECHNICAL REPORT

Constant-Probability Crack Growth Curves

H. Ghonem

Mechanics of Solids Laboratory

Department of Mechanical Engineering and Applied Mechanics

University of Rhode Island, Kingston, RI 02881, USA

Abstract

This paper details a stochastic, time-inhomogeneous model that serves as a theoretical basis for the prediction of crack growth and its variability under constant-amplitude loading. Crack evolution is described as a set of constant probability curves, each of whose points possess equal probability of advancing from one position to another forward position. This probability is governed by a transition intensity parameter for which two mathematical interpretations are examined. A simplified crack growth rate equation, employing one of the definitions, is derived and applied to A17075-T6 material for different loading conditions. Results of this application are compared with those experimentally obtained.

Introduction

The work of Ghonem et al (1,2) describes a probabilistic crack growth model based on the assumption that fracture history can be established by employing a particular discontinuous Markovian process which takes into account the fundamental aspects of the crack growth mechanism. This approach leads to the description of the sample curve of the crack growth process

in terms of a constant-probability criterion. When considering that the crack growth curve given by any continuum crack growth model coincides with the median growth curve, the probabilistic model would then be sufficient to describe the evolution of the crack length and associated scatter at any stress level (3,4). The present paper is an attempt to extend the concepts of the model by including a different definition for the transition intensity probability of the growth process. This will lead to the derivation of a simple and explicit probabilistic crack growth rate equation similar in structure to the Paris-Erdogan equation.

The first part of the paper focuses on the constant probability crack growth curve concept and its model derivation, while the second part will deal with the application of the proposed law.

Model

The basic model is based on the assumption the crack front in the crack propagation stage, as shown in Figure 1, can be approximated by a large number M of arbitrarily chosen points α, α=1,.....,M. Each of these points in terms of the theory of probability, identifies a statistical "trial" or "experiment" conductaed under identical conditions. The fracture state of the αth trial at cycle "i" is given by the crack length or random variable ${}^{\alpha}a_i\ (x_1,x_2,x_3)$ whose evolution with time shall then be established.

The following observations can be made regarding ${}^{\alpha}a_i$:

1- the evolution of ${}^{\alpha}a_i$ in the x_1, x_2 and x_3 directions are statistically independent of each other.

2- the statistical evolution of ${}^{\alpha}a_i$ (x_1) is different from those of ${}^{\alpha}a_i$ (x_2) and ${}^{\alpha}a_i$ (x_3) in that the former consistently increases while the latter may be described as a type of random-walk phenomenon.

3- for an external load applied in the x_1 direction, the crack evolution in the x_2 asnd x_3 directions are orders of a lesser magnitude than that in the x_1 direction.

On the basis of these obsesrvations this model is limited to the evolution of ${}^{\alpha}a_i$ (x_1) by assuming that the crack growth distributions of ${}^{\alpha}a_i$ (x_2) and ${}^{\alpha}a_i$ (x_3) can be described by Dirac-Delta functions. So, ${}^{\alpha}a_i$ will hereafter be referred to as a_i.

Due to the built-in limitations of all experimental techniques in crack measurement, the observed value of a_i can only be specified within a range of:

$$x < a_i < x + \Delta x$$

where Δx is the experimental error and x is the crack position calculated as (see Fig. 2):

$$x = r\,\Delta x \qquad ; \qquad r_o < r < r_f \tag{1}$$

Here "r" identifies the observable zone or state along the fracture surface; r_o is the initial propagation state, r_f is the

state just prior to catastrophic failure of the specimen and r_1, r_2,....., r_{f-1} are the intermediate zones, all zones having the same width.

Given that the crack is in state r, then after i cycles from the instant of reaching r, one of two events will occur. Either a_i will remain in state r (event ${}^{r}E_i$) or a_i will not be in state r (event ${}^{s}E_i$). The following points should now be noted.

a) The crack propagation process is irreversible (i.e. there is no rewelding of crack surfaces.) Hence the crack, if it is not in state r after i cycles, must exist in a state greater than r.

b) Since it is not possible for the crack to propagate from one state to another state without penetrating the adjacent one, the crack can be identified by the number of cycles (i) required to advance from a given state to the immediately following state.

Based on these observations, events ${}^{r}E_i$ and ${}^{s}E_i$ can be seen as elements of a measurable space (Ω) (see Reference (3)) and the following definition of the probability measure of a_i becomes possible. At any fatigue cycle i, the probability that a_i is in state r, i.e. the probability of ${}^{r}E_i$, is defined as:

$$P\{a_i \in {}^{r}E_i\} = P\{x < a_i < x+\Delta x\} \qquad (2)$$

$$\text{i.e.} \quad P({}^{r}E_i) = P_r(i) \qquad (3)$$

Therefore, the probability of a_i not falling within r, i.e. the probability of ${}^{s}E_i$ is,

$$P({}^{s}E_i) = 1 - P_r(i) \qquad (4)$$

It can be seen that, $P_r(i)$ should continuously decrease as the number of cycles increases. Before proceeding further to identify the parameters that define $P_r(i)$, it is necessary to make these comments.

Under conditions of constant amplitude loading, where no overloading effects are considered, the growth of a crack from a particular state depends only on its present mechanical and microstructural details. More specifically, the probability of a_i propagating from state r to r+1 in the cycle interval (i, $i+\Delta i$) depends on the event (${}^{r}E_i$) and is independent of the events prior to i, (${}^{r}E_j$, $j<i$). to elaborate, let (${}^{r+1}E_i$) be the event of a_i jumping to (r+1) from r in the interval (i, $i+\Delta i$). This represents a future event if (${}^{r}E_i$) is an event in the present. Clearly, the future event is conditional on the occurrence of the present event. Given that the present has occurred, the probability of the future is not affected by the probability of the occurrence of the past (${}^{r}E_j$, $j<i$). Also, the occurrence of (${}^{r}E_i$) precludes the occurrence of the (${}^{s}E_j$, $j<i$, $s>r$) due to the irreversible nature of the crack growth process.

The above feature is similar to that of a pure birth Markovian process in which the future is determined only by the

present and not by the past, and in which the discrete space variable never decreases in magnitude with increase of time. This analogy helps to define a transition probability that is also a Markovian property and introduce the conditional probability function that governs the crack growth process as:

$$P\{{}^{r+1}E_i \;/\; {}^{r}E_i,\ldots,{}^{r}E_j,\ldots {}^{r}E_o\} = P\{{}^{r+1}E\ \Delta i \;/\; {}^{r}E_i\}$$

$$= P_{rt}(i) \quad ; \quad i\ j \qquad (5)$$

where $P_{rt}(i)$ is the transition probability linking the probability measures of two consecutive states "r" and "t" (t = r+1) along the fracture surface and "/" denotes the conditional probability. This property, together with the evolution of a_i within the two event sample space (Ω), describes a discrete space continuous time Markov process.

Since the analogy to the Markovian process has been shown, the criteria attached to this process can be assumed to be valid for the crack growth as well.

They are:

1- The probability a_i propagating to a state different from r in Δi cycles, where Δi is very small, after i cycles elapse in state r is:

$$P_s(\Delta i) = P[{}^{t}E\ \Delta i \;/\; {}^{r}E_i] + 0(\Delta i)$$

$$= \lambda_r\ \Delta i + 0(\Delta i); \quad t=r+1 \qquad (6)$$

Here, λ_r is a positive variable indicating the

probability transition rate. It describes the transition rate from state r to $r+1$ in i cycles.

In this analysis, λ_r is assumed to be a material parameter which in addition to being a function of crack position r, should depend explicitly on both initial cycle i, and duration Δi. The propagation process thus becomes time-inhomogeneous.

2- The corresponding probability that a_i will be in state r during the cycle interval Δi is:

$$P_r(\Delta i) = P\{{}^{r}E_{\Delta i} \,/\, {}^{r}E_i\} + O(\Delta i)$$
$$= (1 - \lambda_r \Delta i) + O(\Delta i) \qquad (7)$$

3- The probability that a_i is in a state different from $r+1$ is:

$$P_{rt}(\Delta i) = P\{{}^{t}E_{\Delta i} \,/\, {}^{r}E_i\}$$
$$= O(\Delta i) \quad ; \quad t \neq r+1 \qquad (8)$$

The time interval Δi is so small that the probability of advancing from r to a state greater than $r+1$ is almost zero. By definition, $O(\Delta i)$ is such that,

$$\lim_{\Delta i \to 0} \frac{O(\Delta i)}{\Delta i} = 0$$

Now, let

$$A = {}^{r}E_i \quad \text{and}$$

$$B = {}^{r}E_{\Delta i}$$

Then

$$A \cap B = {}^{r}E_{i+\Delta i}$$

Since

$$P(A \cap B) = P(B/A) \cdot P(A)$$

Therefore

$$P\{{}^{r}E_{i+\Delta i}\} = P\{{}^{r}E_{\Delta i} / {}^{r}E_i\} \cdot P\{{}^{r}E_i\} \tag{9}$$

Substituting Equations (6), (7) and (8) in (9) we get,

$$P\{{}^{r}E_{i+\Delta i}\} = (1 - \lambda_r \Delta i) \cdot P\{{}^{r}E_i\} + 0(\Delta i) \tag{10}$$

which can be written as

$$P_r(i+\Delta i) = (1-\lambda_r \Delta i) \cdot P_r(i) + 0(\Delta i) \tag{11}$$

By transposing the term $P_r(i)$, dividing by Δi and passing to the limit $\Delta i \to 0$, equation (11) becomes

$$\frac{dP_r(i)}{di} = - \lambda_r P_r(i) \tag{12}$$

The solution of this equation is:

$$\ell n\, P_r(i) = - \int \lambda_r \, di + L_1 \tag{13}$$

where L_1 is a constant.

This equation describes the crack growth probability from state r, after i cycles elapse, in terms of the constant L_1 and the transition rate λ_r which is discussed below.

The parameter λ_r was introduced in this model as the transition intensity by which a_i propagates from one state to the next. Adopting the notion that the crack growth process is a discrete one, the crack transition from a specific state can be viewed as being governed by a critical threshold energy at the crack tip. When such a threshold (which is environmental, material, stress and crack-length dependent) is satisfied by cyclic energy accumulation, a crack tip transition can be said to occur. Therefore the larger the cycle duration associated with the crack in a specific state, the greater the probability that the propagation threshold is satisfied and the greater the probability that the crack advances to the following state.

The transition intensity, λ_r, can be assumed to have several physical interpretations, however, the primary concern at this point is whether λ_r is a material property present only when there is application of cyclic loads or whether it exists even when there is no cycling.

If λ_r is a property that owes its existence to cyclic loading, then it could represent a dislocation accumulation rate, a microvoid growth rate, a ductility exhaustion rate or a rate at which any physical phenomenon occurs in the grain structure of a polycrystalline material to aid the propagation of a crack. In that case, the magnitude of λ_r should be zero at any instant

there is no cycling. Specifically, its magnitude should be equal to zero at i=0, the instant at which the load cycling is about to begin, after the crack has reached a particular state, r. Keeping in mind the fact that λ_r should monotonically increase with i, the following expression for λ_r can then be chosen.

$$\lambda_r(i) = L(r)\, i^{\alpha(r)} \tag{14}$$

where L(r) and $\alpha(r)$ are functions of the crack state.

If, on the other hand, λ_r is a property present even when there is no cyclic loading, the physical analogy for λ_r would be completely different. λ_r would then represent a dislocation density in the microstructure or a microvoid density in the microstructure of a material. Thus while the property λ_r does increase in magnitude during cycling, it does not cease to exist when the cycling is absent. Hence, from this point of view, λ_r should have a value corresponding to i=0, the instant at which the cycling is about to begin after the crack has reached a specified state, r. The following expression could then be considered.

$$\lambda_r = L(r)\, e^{\alpha(r)i} \tag{15}$$

From a purely mathematical point of view expression (15) was first selected to be utilized in the present model. By substituting Equation (15) in (13), it yields:

$$\ell n P_r(i) = - B\, e^{Ci} + L_1 \qquad (16)$$

where $B = L/C$

The upper and lower limits of $P_r(i)$ in the above equation are:

$$1 \geq P_r(i) \geq 0 \qquad (17)$$

The form of equation (15) suggests that i has a lower boundary that satisfies the upper limit condition of $P_r(i)$. Equation (16) thus becomes:

$$\ln P_r(i) = B(e^{CI_o} - e^{Ci}) \qquad i > I_o$$

$$= 0 \qquad i \leq I_o \qquad (18)$$

where the parameters B, C and I_o, the incubation time, are found to be:

$$B = C_1\, a_r^{n_1} \quad ; \qquad (19)$$

$$C = C_2\, a_r^{n_2} \qquad (20)$$

and $$I_o = C_3\, [a_{r-1}^{n_3} - a_r^{n_3}] \qquad (21)$$

C_1, C_2, C_3, n_1, n_2 and n_3 are material-, stress- and environment-dependent parameters.

The application of the above equation (18) to different steel and aluminum alloys is detailed in Ref. (3).

In this paper the interpretation concerning λ_r, as given in Equation (14), will be examined. By substituting this equation in (13) and setting the upper and lower limits of $P_r(i)$ to:

$$1 \geq P_r(i) \geq 0$$

one can arrive at the following solution

$$\Delta i = A(-\ln P_r(i))^{\beta} \tag{22}$$

where $A = \left(\frac{1+\alpha}{L}\right)^{\frac{1}{1+\alpha}}$

and $\beta = \frac{1}{1+\alpha}$

A and B are considered here to be material-, stress- and crack position dependents.

The above equation identifies the duration of fatigue cycles required for a crack at position r to propagate with a specific constant probability $P_r(i)$, to a position r+1 along the fracture surface. By calculating such durations for states r_1 to r_{f-1}, the history of the entire constant-probability crack growth curve can be obtained. If an assumption is made that the crack growth curve generated by a continuum model coincides with the median growth curve, i.e., the $P_r(i) = 0.5$ curve, parameters A and β can be determined and Equation (22) becomes fully defined for a particular material and a particular constant amplitude stress condition. The work described below explains the procedure for determining the expressions of both A and β.

Following the approach detailed in Ref (3), work of Virckler et al (5), which combines crack growth data of 68 replicate tests of Al2024-T3, shown in Figure 3(a) was arranged in 9 constant probability crack growth curves as shown in Figure 3(b). Data points representing cycle intervals corresponding to similar discrete crack positions along three different constant-probability curves; $P_r(i) = 0.05$, 0.5 and 0.95, were used as input to Equation (22) to determine the parameters A and β. Using curve regression analysis parameter β was found to be constant for all state positions with a value of 0.166. The parameter A varied as function of r in a pattern shown in Figure 3 which is fitted into the form:

$$A = 1.5 \times 10^7 \left((r-1)^{-1} - r^{-1}\right) \qquad (23)$$

Similarly, data of Yang et al (6), Figure (4), which consist of the distribution of crack size as function of load cycles for IN-100 tested for two different load conditions, were used to obtain the expressions for A and β. These expressions were obtained as:

Test Condition I

$$A = 4.3 \times 10^6 \left((r-1)^{-0.70} - r^{-0.7}\right)$$
$$\beta = 0.155 \qquad (24)$$

Test Condition II

$$A = 4.06\times10^{6}\ ((r-1)^{-1.4} - r^{-1.4})$$

$$\beta = 0.266 \qquad (25)$$

By observing the forms of A and β, as expressed in Equations 23-25, obtained from two different types of alloys, one can conclude that, while β seems to be a constant which depends mainly on the material and stress condition, a general form of A depends on the crack position and can be written as:

$$A = C_1((r-1)^{\gamma} - r^{\gamma})$$

where C_1 and γ are material- and stres-dependent parameters. Therefore, one can write Equation (21) as:

$$\Delta i = C_1((r-1)^{\gamma} - r^{\gamma})(-\ln P\ (i))^{\beta}$$

$$= \frac{C_1}{\Delta x^{\gamma}}\ [\Delta x^{\gamma}(r-1)^{\gamma} - \Delta x^{\gamma} r^{\gamma}](-\ln P)^{\beta} \qquad (26)$$

since the crack length a_r can be written as $a_r = \Delta x \cdot r$, thus, Equation (26) becomes

$$\Delta i = C_2(a_{r-1}^{\gamma} - a_r^{\gamma})(-\ln P)^{\beta} \qquad (27)$$

where $C_2 = C_1/\Delta x^{\gamma}$. One should remember here that Δi is the number of cycles counted from the instant the crack tip reaches state r and P is the probability that the crack will not propagate from state r to the following state within Δi cycles.

For the same value of $P_r(i)$, i.e. operating on a single crack growth curve, Equation (27) can be manipulated as follows:

$$\Delta i_1 = i_1 - 0 = C_2(a_o^{\gamma} - a_1^{\gamma})(-\ln P)^{\beta}$$

where a_o is a constant that represents the initial crack length.

$$\Delta i_2 = i_2 - i_1 = C_2(a_1^{\gamma} - a_r^{\gamma})(-\ln P)^{\beta}$$

.....

.....

.....

$$\Delta i_r = i_{r-1} - i_r = C_2^{\gamma}(a_{r-1} - a_r^{\gamma})(-\ln P)^{\beta}$$

By summing $\Delta i_1 + \Delta i_2 + \ldots + \Delta i_r$ one obtains

$$i_r = C_2(a_o^{\gamma} - a_r^{\gamma})(-\ln P)^{\beta}$$

Differentiating both ends w.r.t. i; thus:

$$1 = C_2 \left(-\gamma\, a_r^{\gamma-1} \frac{da}{di}\right)(-\ln P)^{\beta}$$

This equation can be rearranged as:

$$\frac{da}{di} = C_3\, a^{\delta}\, (-\ln P)^{-\beta} \qquad (28)$$

where $C_3 = \frac{-1}{C_2\, \gamma}$

and $\delta = 1 - \gamma$

By multiplying and dividing Equation (28) with $\Delta\sigma_0^{2\delta}\ \pi^{\delta}$; where $\Delta\sigma_0$ is the stress range, one can obtain:

$$\frac{da}{di} = C\ \Delta\sigma_0^{2\delta}\ \pi^{\delta}\ a^{\delta}\ (-\ln P)^{-\beta} \qquad (29)$$

where $C = C_3/\Delta\sigma_0^{2\delta}\ \pi^{\delta}$

Equation (29) could then be written as:

$$\frac{da}{di} = C_{\ell}(\Delta K)^{\delta}\ (-\ln P)^{-\beta} \qquad (30)$$

which represents a crack growth rate equation for a crack progressing from one state to the following state along the fracture surface with a constant probability P.

From the experimental work of Yang et al (5) and Ghonem and Dore (3), it is observed that the degree of scattaer of the constant probability curves measured as the number of cycles that separates the $P_r(i) = 0.95$ curve from the one of $P_r(i) = 0.05$ at the same crack length decreases as the maximum applied stress, S_{max}, increases. One can assume that, at very high values of S_{max}, the influence of the material microstructure and other test conditions would decrease to the extent that all probability crack-growth-rate curves would be described by a single curve. At this loading level, paramter β is equal zero, i.e. β follows a pattern which can be simply expressed as:

$$\beta = S_o - \beta_o S_{max} \qquad (31)$$

where β_o is a constant and S_o is related to the maximum stress value at which all probability crack growth curves become one curve. Equation (30) could be written as:

$$\frac{da}{dN} = C_\ell (\Delta k)^\delta (-\ln P)^{S_o - \beta_o S_{max}} \qquad (32)$$

As mentioned before a basic assumption in the work of Ref. (2) is that the median of the constant probability crack growth equation, i.e., the curve with $P_r(i) = 0.5$, can be described using a continuum crack growth law. By invoking this assumption the validity of Equation (30) could be examined using results of tests carried out on Al 7075-T6 specimens (3). In this work the crack length versus number-of-cycles was obtained for three different stress conditions. Each condition was tested by using sixty identical center-notched flat specimens (320.67 x 50.8 x 3.175 mm) resulting in sixty crack-growth curves, each consisting of 256 points generated through the use of an automated photographic technique detailed in Ref (3). The results of this study and the corresponding experimental constant probability crack growth curves are shown in Figures 5-8. Following an argument discussed in the above mentioned study, Forman's Equation (6) was selected as a suitable continuum crack-growth law since it recognizes the effect of the stress ratio R and is well documented for Al7075-T6; it is written as

$$\frac{da}{di} = \frac{C \ \Delta K^m}{(1-R)(K_c - K_{max})} \qquad (33)$$

where

$K_c = 74$ MPa-$m^{\frac{1}{2}}$

$C = 1.63 \times 10^{-17}$

$m = 3.065$

The results of the comparison of this equation with those experimentally obtained for $P_r(i) = 0.5$ are shown in Figure 9; they indicated close agreement.

The above equation could now be equated to Equation (30) in which $P_r(i) = 0.5$. In this equality the parameter δ is set equal to m of Formann equation, i.e., $\delta = 3.065$. Using an iterative numerical technique that employs the Newton-Raphston method, values of C_ℓ and β for the three different load conditions were obtained:

	test condition I	test condition II	test condition III
C_ℓ	2.64×10^{-4}	1.65×10^{-4}	1.42×10^{-4}
β	0.195	0.203	0.299

The parameters C_ℓ and β were then substituted in Equation (30) to generate, for each load condition, the entire spectrum of the

constant probability crack growth rate curves. These curves were compared to those experimentally obtained in Figure 8. Results of this comparison, in the form of percentage-of-error of number-of-cycles corresponding to a similar crack length, are summarized in Figures 10. These results show that the error of the model under test conditions I, II and III are ±2.5%, ±5% and ±8% respectively. This degree of error is similar to that obtained when λ_r is expressed by equation (15), see Ref. (3). Furthermore, a comparison between both the theoretical and experimental cumulative distribution function for selected crack lengths, at the three different loading conditions, are shown in Figure 11; they indicate a very close agreement.

Summary

This paper has outlined the principle of a stochastic model aimed at describing crack growth and its variability due to random characteristics of the microstructure of polycrystalline solids. The model was built by developing an analogy to a discontinuous Markovian process. This treatment leads to the calculation of the cycle duration required for a point along the crack tip to advance with a particular probability to a forward state along the fracture surface. This probability is governed by a transition intensity parameter, λ_r, which is viewed here as material- and cycle-dependent. In the absence of a definite physical interpretation of this parameter, it has been given two mathematical expressions which differ in that one expression, λ_r, possesses a value when Δi approaches zero, while in the other

expression λ_r becomes zero as $\Delta i \to 0$. The paper examined the latter condition which then led to the derivation of a crack growth rate equation in which a probability term is explicit. Comparison of the results of this equation, when applied to A17075-T6 for three different loading conditions, indicates agreement with experimental results obtained by the author for the same loading conditions.

References

1. H. Ghonem and J.W. Provan, Micromechanics theory of fatigue crack initiation and propagation, Engrg Fracture Mech, 13, 963-977 (1980).
2. H. Ghonem and S. Dore, Probabilistic description of fatigue crack propagation in polycrystalline solids, Engrg Fracture Mechanics, 21, 1151-1168.
3. H. Ghonem and S. Dore, Probabilistic description of fatigue crack growth in aluminum alloys, AFOSR-83-0322 (April 1986).
4. H. Ghonem and S. Dore, Experimental study of the constant-probability crack growth curves under constant amplitude loading, Engrg Fracture Mechanics, 27, 1-25 (1987).
5. D.A. Virckler, B.M. Hillberry and P.K. Goel, The statistical nature of fatigue crack propagation, J. Engrg Mater. Technol. 101, 148-153 (1979).
6. J.N. Yang and R.C. Donath, Statistics of crack growth of a super-alloy under sustained load, J. Engrg Mater. Technol. 106, 79-83 (1984).

7. R.G. Forman, V.E. Kearney and R.M. Engle, Numerical analysis of crack propagation in cyclic loaded structures, J. Basic Engrg, 459-464 (September 1967).

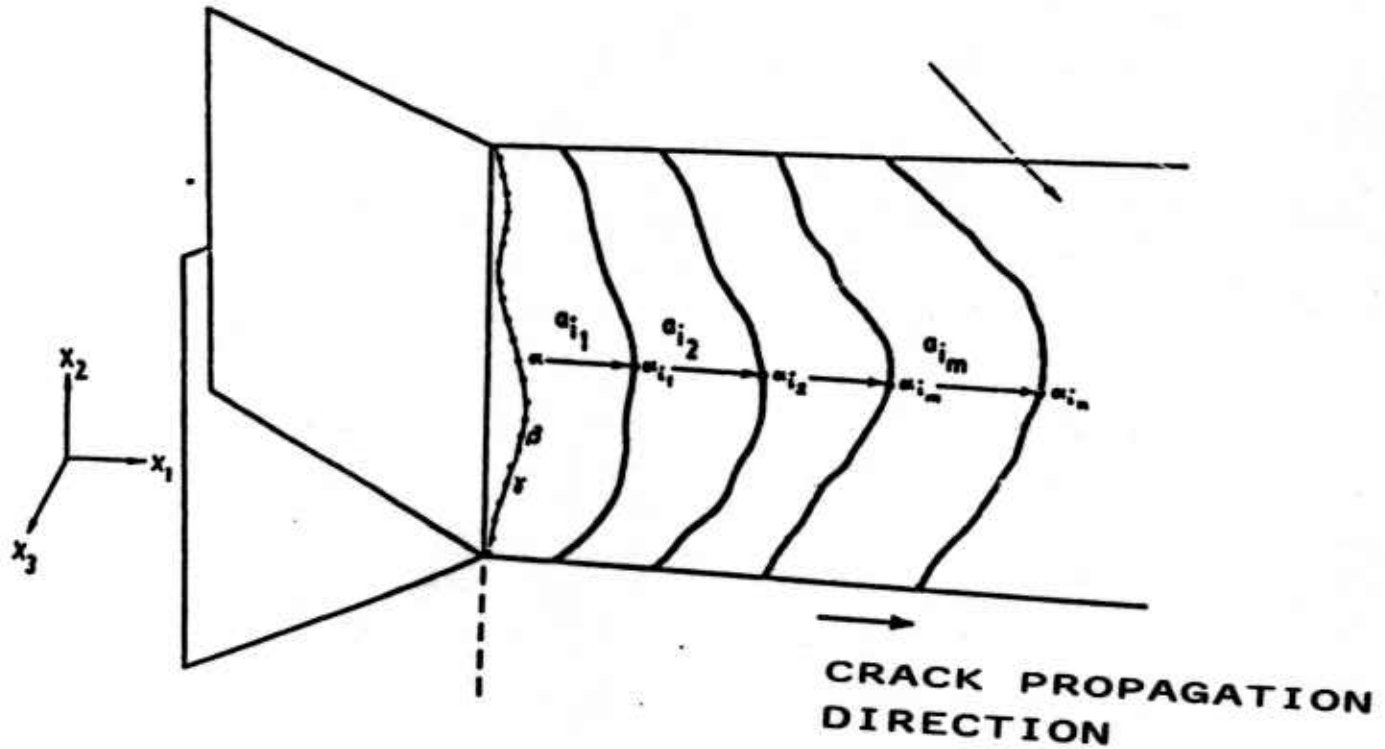

FIGURE 1: Schematic of Mode I Crack Propagation Fracture Surface

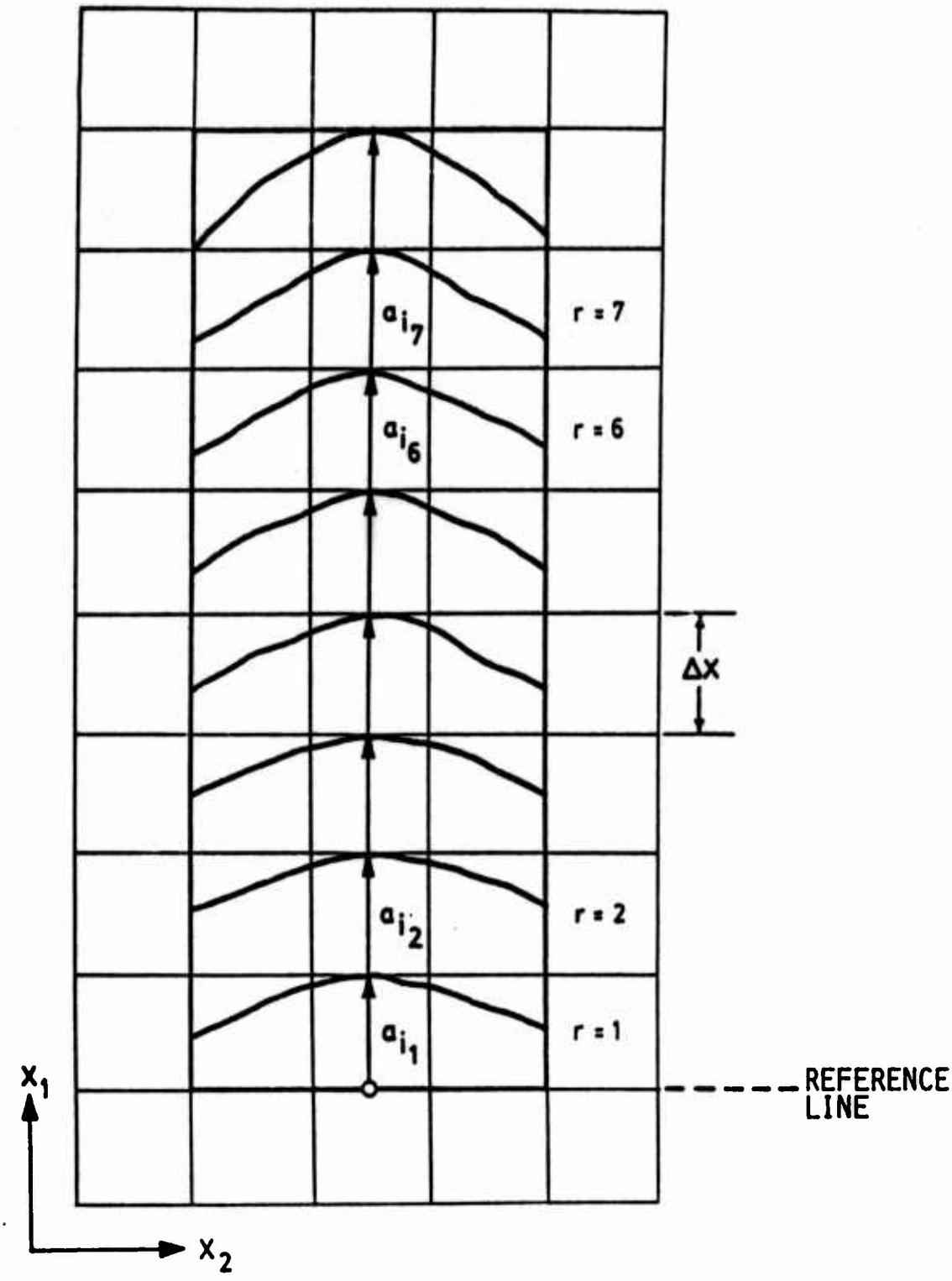

FIGURE 2: Schematic of the Proposed Fatigue Crack Propagation

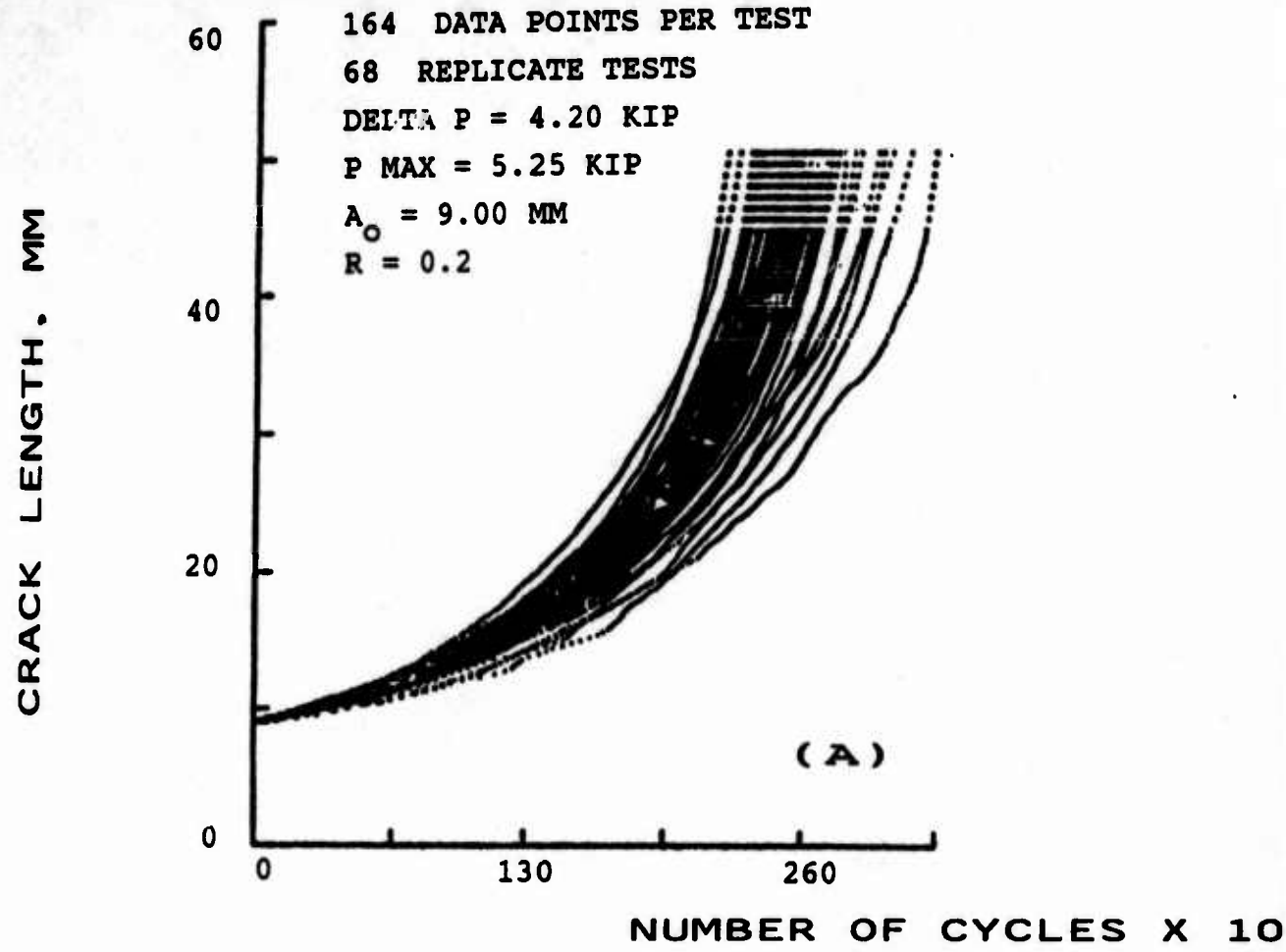

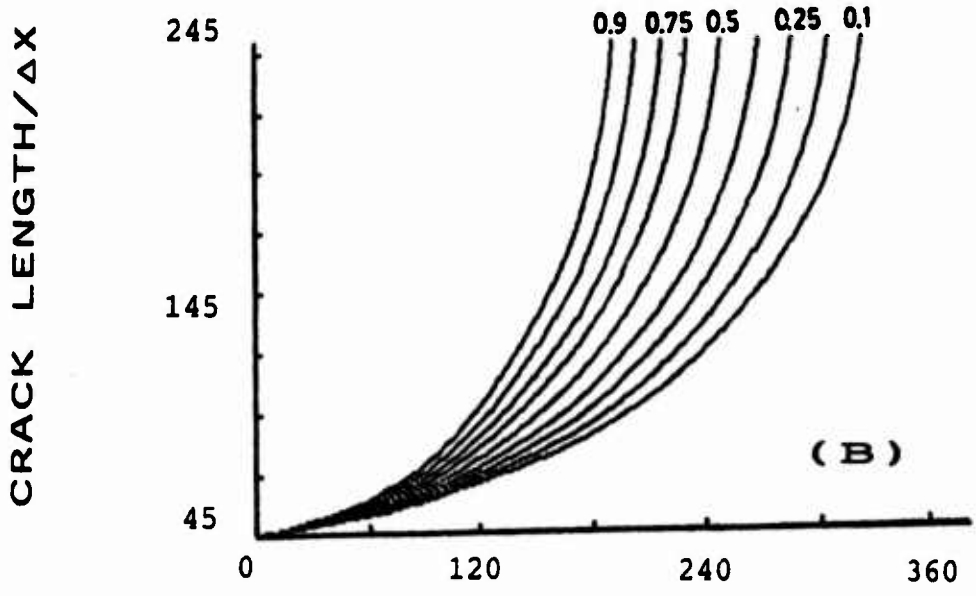

FIGURE 3(a): Replicate of Crack-Length versus Number of Cycles Data Set from Virckler's Study

(b): Experimental Constant-Probability Crack Growth Curves Generated from the Data in Figure 3(a)

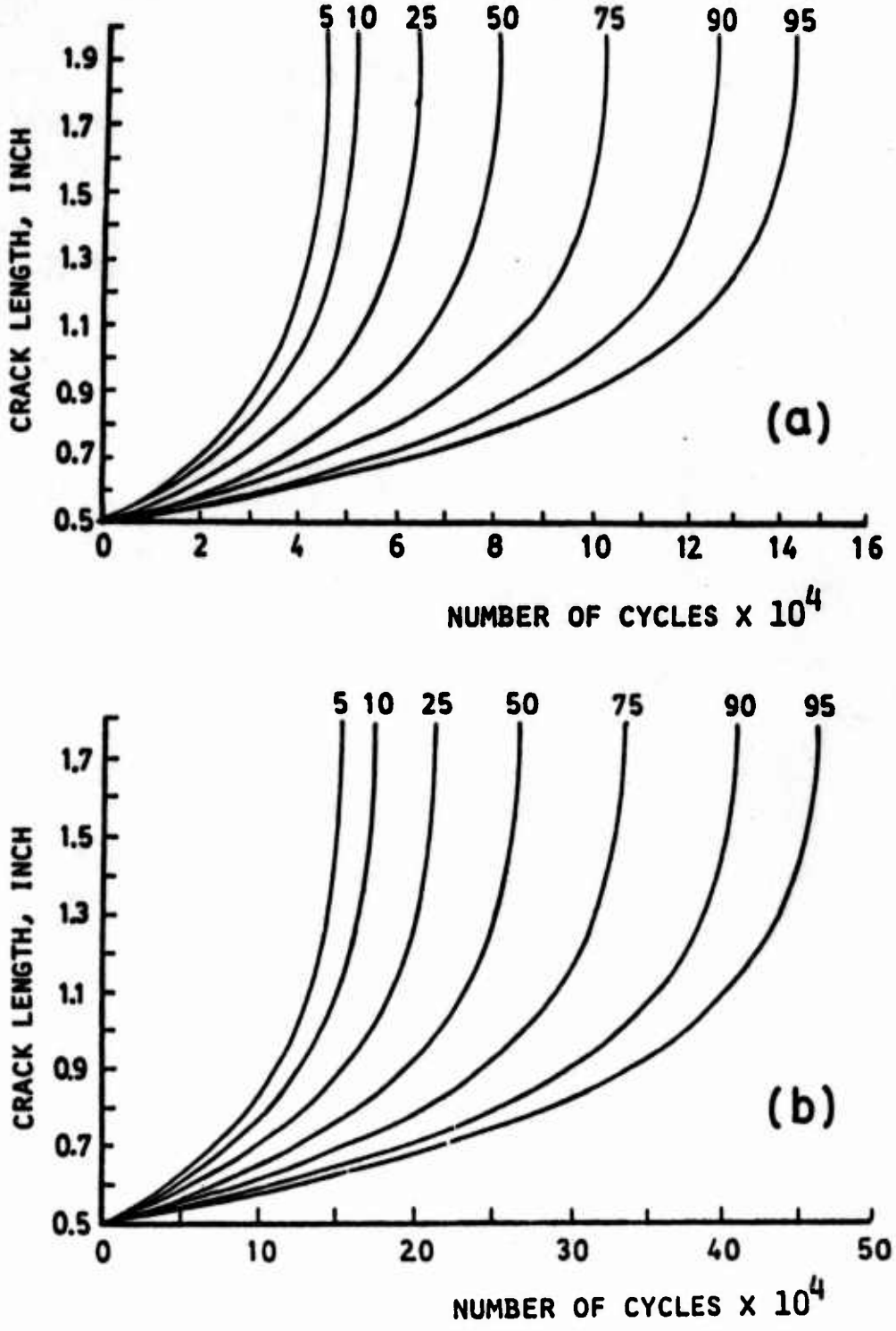

Figure 4. Experimental constant-probability growth curves for (a) Test condition I and (b) Test condition II [6]

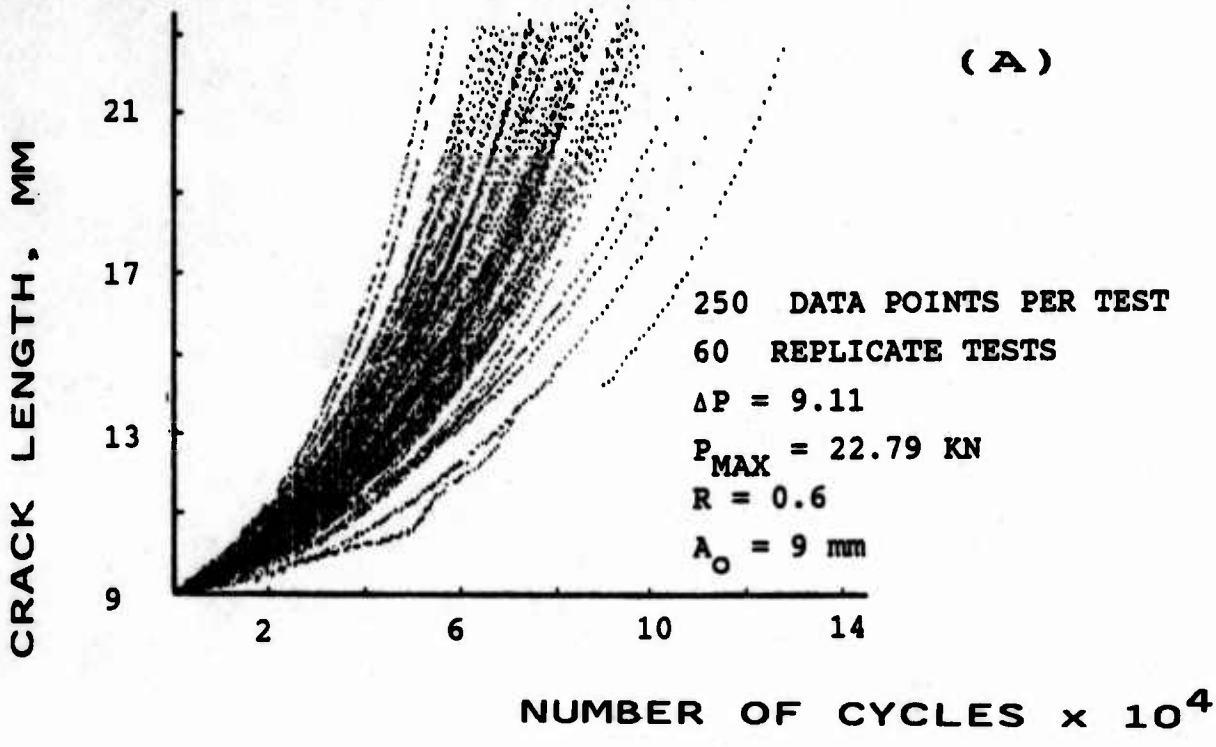

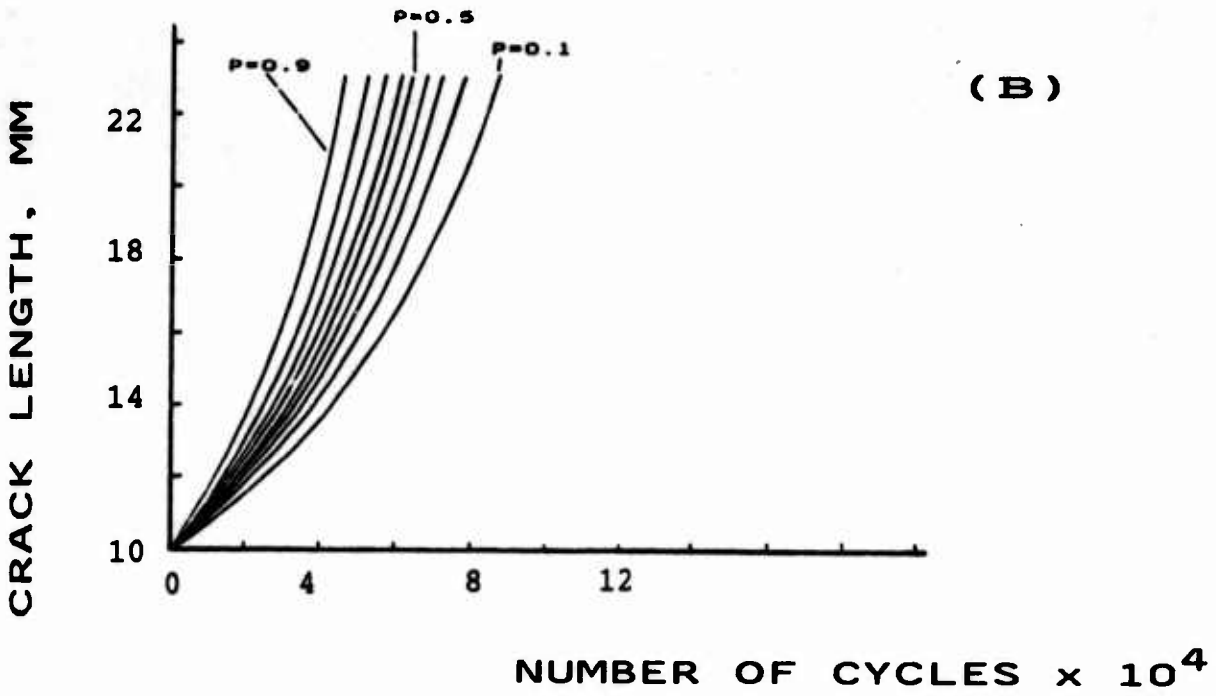

FIGURE 5(a): Crack-Length Versus Number-of-Cycles for Test Condition (I)

(b): Corresponding Constant Probability Crack Growth Curves

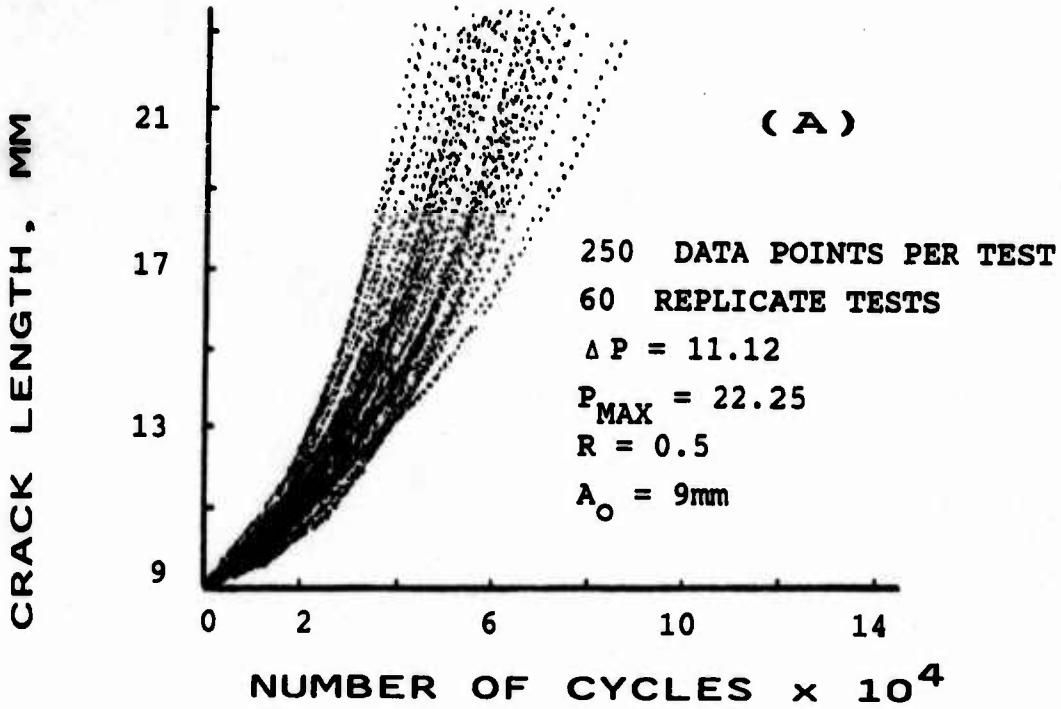

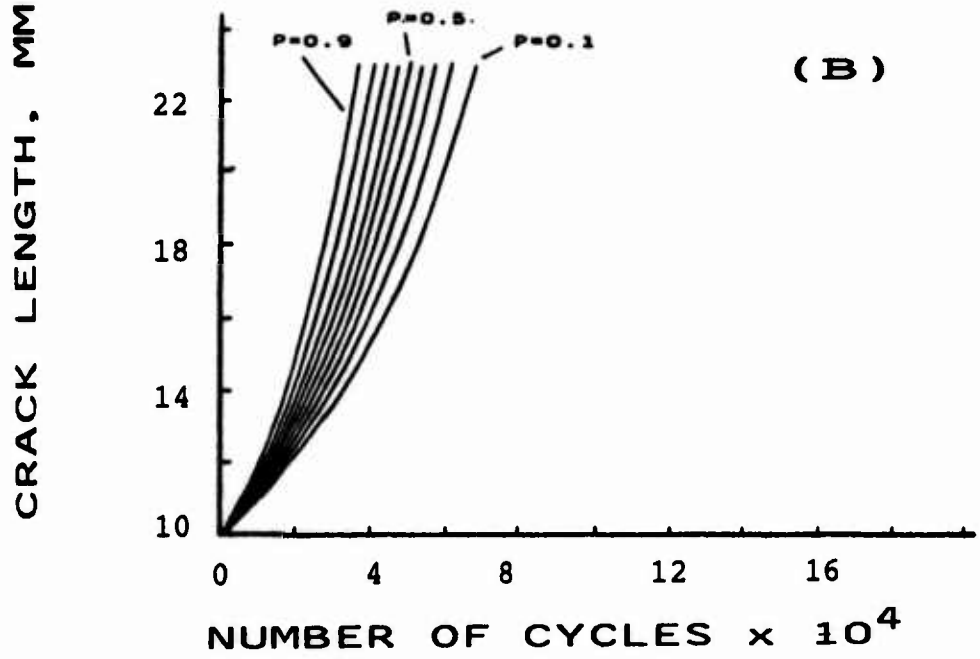

FIGURE 6(a): Crack-Length Versus Number-of-Cycles for Test Condition (II)

(b): Corresponding Constant Probability Crack Growth Curves

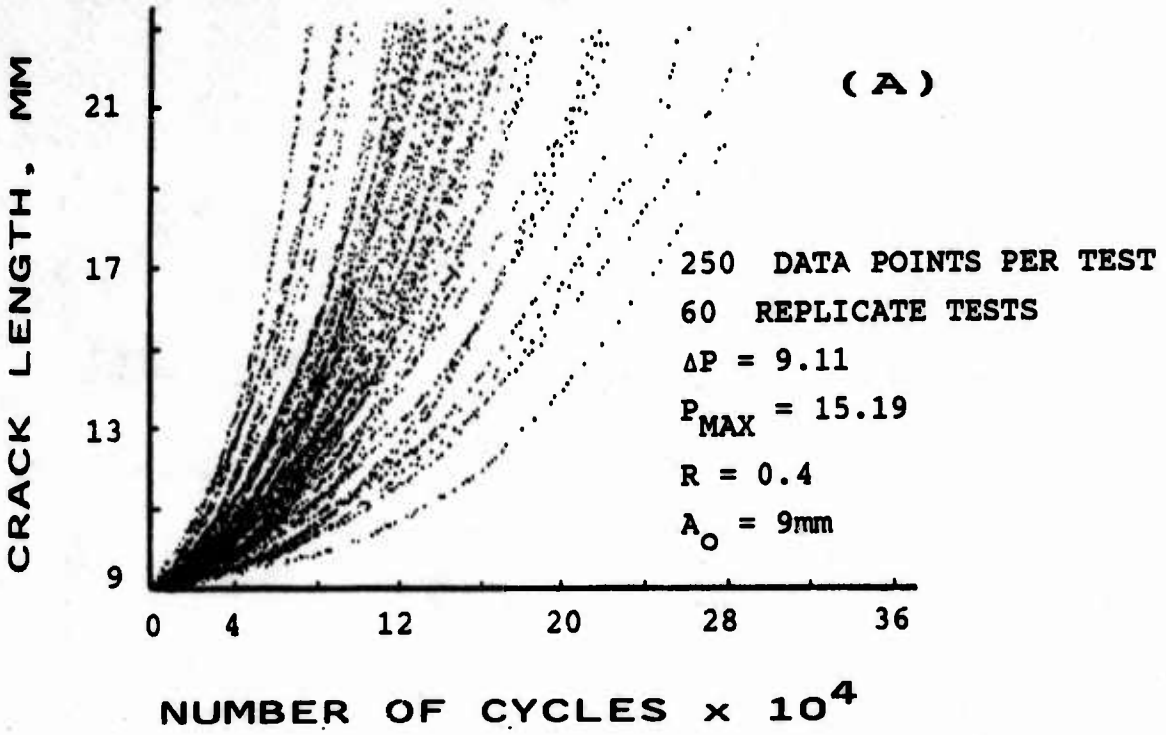

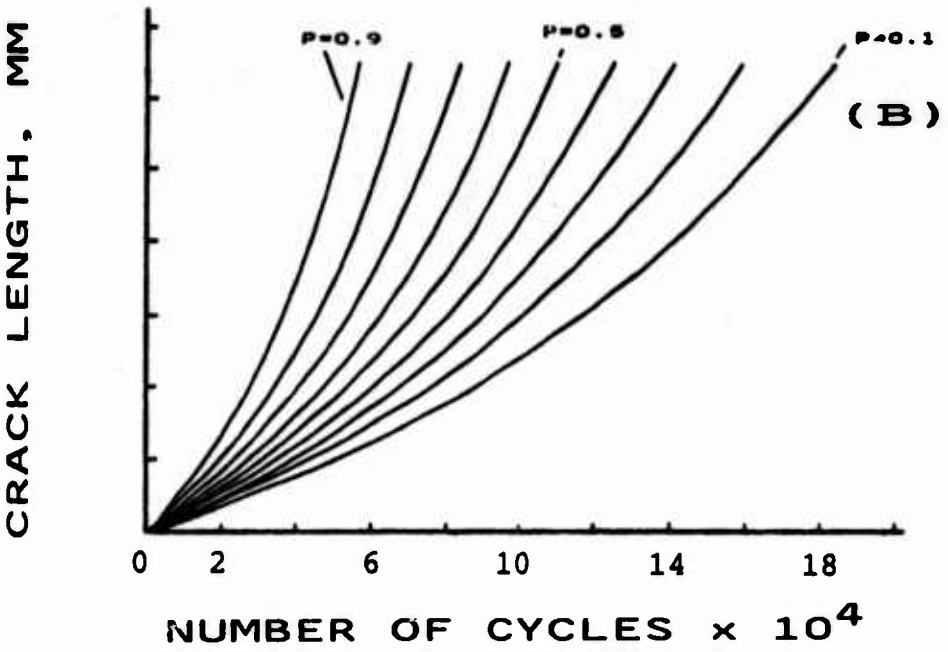

FIGURE 7(a): Crack-Length Versus Number-of-Cycles for Test Condition (III)

(b): Corresponding Constant Probability Crack Growth Curves

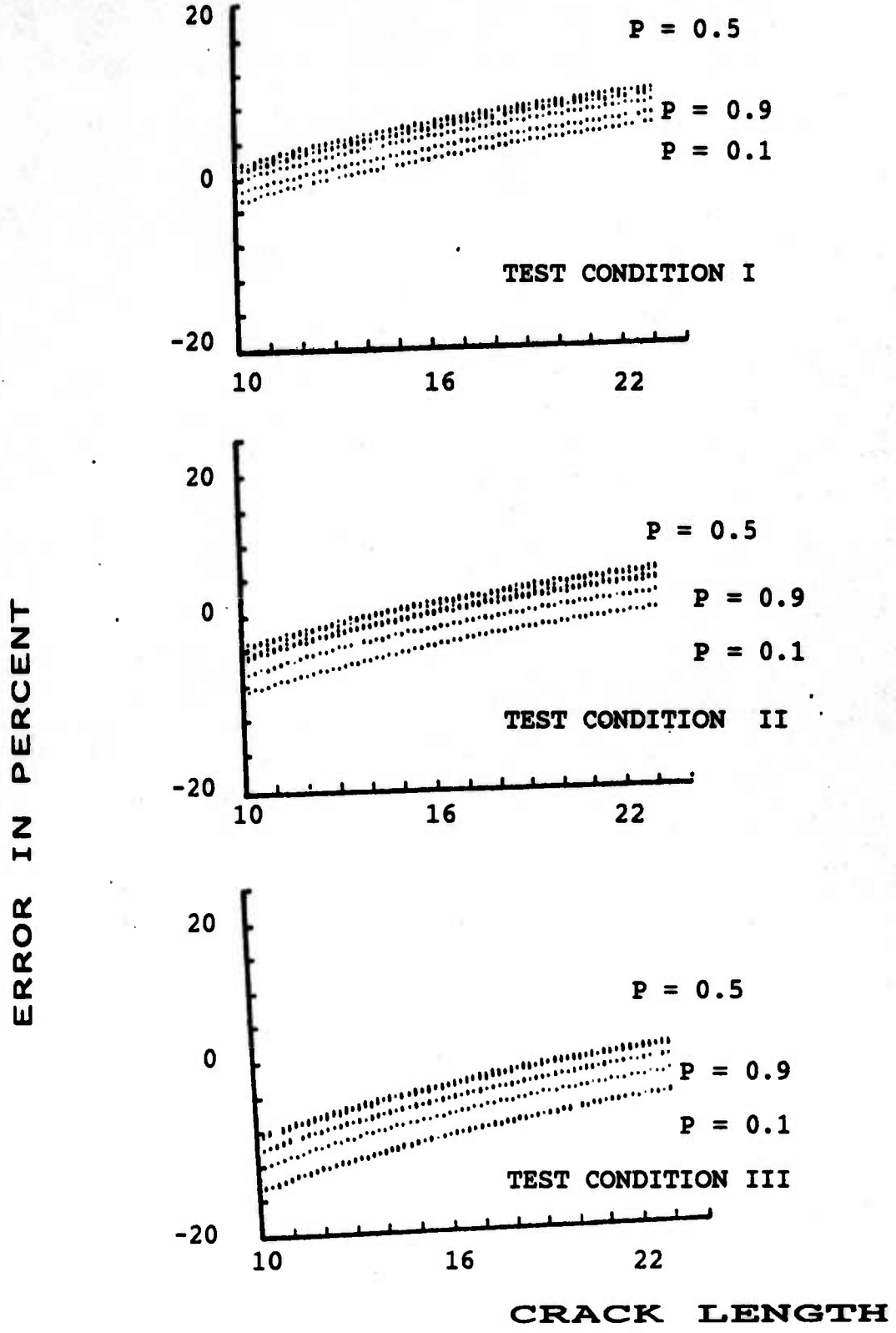

FIGURE 1): Error in Percent of the Proposed Model for the Three Test Conditions

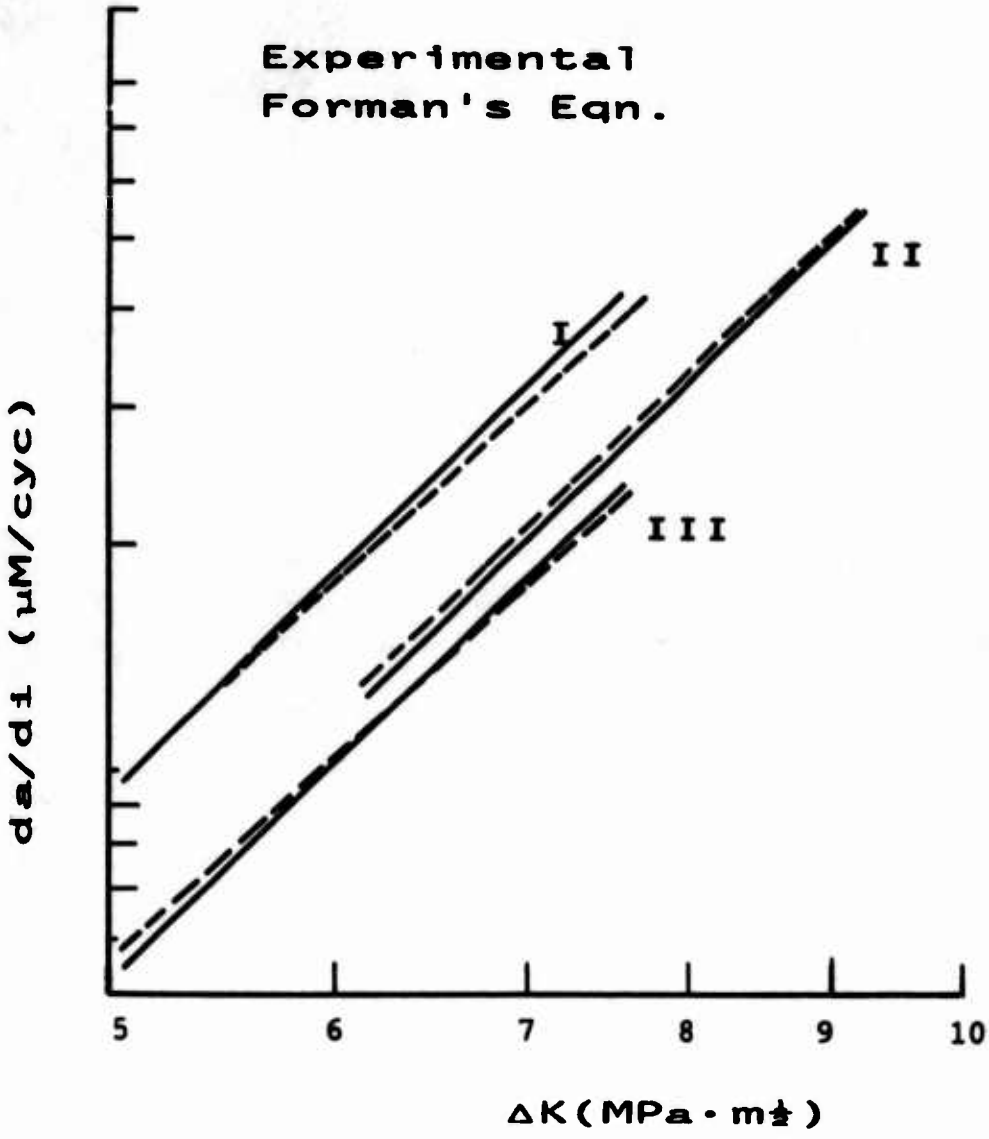

FIGURE 9: Comparison Between Median Curves Obtained Experimentally and Those Calculated Using Forman's Equations

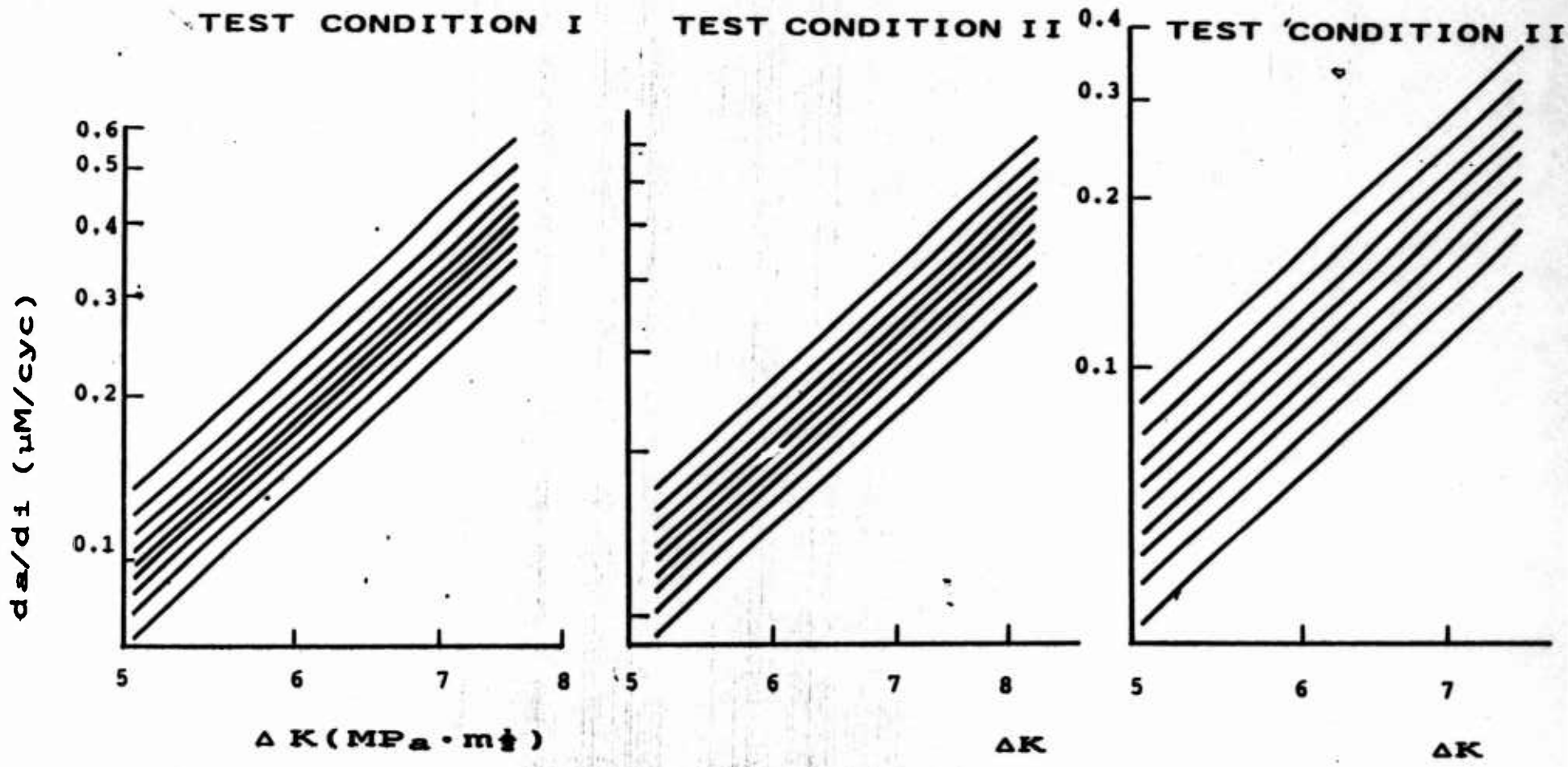

FIGURE 8: Experimental Crack Growth Rate versus Δ K for the Three Test Conditions Shown in Figs. 5-7.

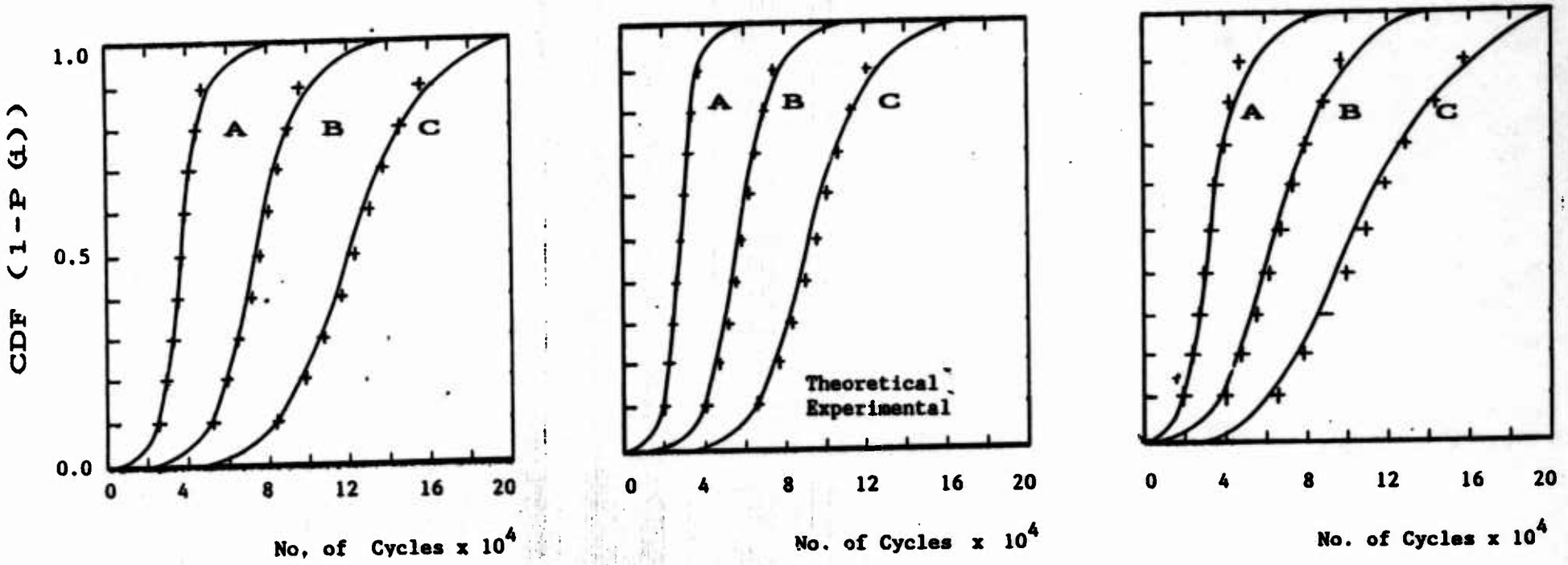

FIGURE 11: Cumulative Distribution Functions versus Number of Cycles for Three Crack Length Positions A = 12 mm, B = 15 mm and C = 21 mm

Engineering Fracture Mechanics Vol. 27, No. 1, pp. 1–25, 1987
Printed in Great Britain

0013-7944/87 $3.00 + 0.00
Pergamon Journals Ltd.

EXPERIMENTAL STUDY OF THE CONSTANT-PROBABILITY CRACK GROWTH CURVES UNDER CONSTANT AMPLITUDE LOADING

H. GHONEM AND S. DORE
Mechanics of Solids Laboratory, Department of Mechanical Engineering and Applied Mechanics, University of Rhode Island, Kingston, RI 02881, U.S.A.

Abstract — This paper is concerned with the application of a mathematical model that describes the fatigue crack growth evolution and associated scatter in polycrystalline solids. The model has been built on the basis that an analogy exists between a particular discontinuous Markovian stochastic process, namely the general pure birth process, and the crack propagation process. The, crack evolution and scatter were then defined in terms of material, stress and crack-length dependent properties and crack tip incubation time.

The application of the model is carried out by comparing the constant-probability crack growth curves generated for three different load levels with those obtained from testing sixty Al 7075-T6 specimens for each load level. A photographic method was utilized to measure the crack-length in this test program, by recording the residual deformation that accompanies the flanks of the crack during propagation.

INTRODUCTION

PREDICTION OF fatigue crack growth, even under constant amplitude loading, has not been an easy task. This is mainly because the manner in which the various parameters, such as loads, material properties and crack geometries, affect the crack propagation is not clearly understood[1]. This, consequently, had led to a proliferation of hypotheses and laws for describing fatigue crack propagation (see review articles in refs [1, 2 and 3]). Most of these models are based on concepts of the continuum theory with the assumption that cracks propagate in an ideal continuum media. Actual metallic materials, however, are composed of random microstructure described by various microparameters which can seriously affect the growth of a crack in these materials. As a result, the deterministic theories can only be accepted as an approximation of the actual random fatigue crack propagation process.

The use of statistical distributions or probabilistic models thus becomes necessary to make predictions of crack growth more reliable. The search for the "true" statistical distribution has been a difficult task since in any application, the amount of crack-growth data which has been collected for any particular case would not be sufficient to discriminate between the different types of distributions[4]. In addition, when a series of tests on identical specimens is performed to establish the scatter due to material properties, the uncertainties in load values and crack-length measurements are also included in the scatter data. Due to this limitation, it is difficult to isolate the scatter associated with material properties in any experiment. One is also hampered by the lack of an exact physical description of the fatigue process[5]. When taking these two factors into consideration, any probabilistic or statistical model can identify the variability of crack-length only in a comparative sense. This means that the absolute values of the variability at a specific load level predicted by a model may not be equal to those obtained experimentally. However, it is possible for a ratio of variabilities predicted for two different load conditions to be equal to that of the experimental results obtained at the same loading conditions. In this, the experimental errors being independent of the magnitude of the applied loads, are eliminated.

There are basically two kinds of mathematical models in existence to predict the variability in fatigue crack growth. The first employs a statistical approach in which random variables are introduced instead of the constants in the appropriate deterministic crack growth equation. While these models (see, for example refs [6–11]) are simple to use and versatile in application, they possess some disadvantages. First, all of them are based on Paris law[12] where it has been shown that other laws like the Forman's law[13] are more applicable. Secondly, the scatter parameters in these models have no physical description and no attempts have been made to link these parameters to the micro-structural properties. Lastly, though these models generate crack-growth

data that match the experimental data reasonably well in some cases, they do not provide any insight into the nature of the fatigue crack propagation process.

The second approach employs evolutionary methods in which the propagation of the crack is treated in a probabilistic or stochastic sense instead of a statistical one. Making use of a specific probability process, namely the Markovian process, the models with this approach strive to correlate the properties of this process with those of fatigue crack propagation.

Examples of this approach are the models by Ghonem *et al.*[14, 15], Kozin and Bogdanoff[16] and Aoki and Sakata[17]. The major disadvantage in using these models is the lack of crack-growth scatter data for different conditions which would have been helpful to check the validity of the probabilistic assumptions on which these models were built.

The objective of this paper is to examine the results of the stochastic model developed by Ghonem and Dore[15] when utilized for the prediction of the crack growth evolution, in the same material, at different loading conditions. Before proceeding on this application, a brief review of the fundamentals of the model is presented in the next section. This will be followed by the description of the experimental study and detailed analysis of the results.

REVIEW OF THE PROPOSED MODEL

In this model, the fracture surface is divided into a finite number of crack "states" of equal width; a probability space of two events was defined with the condition that the crack is in state *"r"* after i cycles have elapsed from the instant of reaching *"r"*. They are, the event that the crack will remain in the state *"r"* and the event that the crack will not be in *"r"*. Assuming that the crack propagation process is irreversible and utilizing the fact that under conditions of constant amplitude loading the existence of a crack at a particular state depends only on its present mechanical and microstructural details, a definition for the transition probability was arrived at. Using the criteria attached to the discontinuous Markovian process[18], a transition intensity (λ_r) could be defined. In this approach, λ is assumed to be a material parameter which in addition to being a function of the crack position *"r"*, should explicitly depend on both the initial elapsed cycles i and the incremental duration Δi. The propagation process thus becomes time-inhomogeneous. This characteristic is a departure from the works of Ghonem and Provan[14] and Kozin and Bogdanoff[16].

The probability equation was then derived and can be written as:

$$\begin{aligned} \ln P_r(i) &= B(e^{KI_0} - e^{Ki}) \quad ; \quad i \geqslant I_0 \\ &= 0 \qquad\qquad\qquad ; \quad i < I_0 \end{aligned} \tag{1}$$

where i is the number of cycles, B and K are crack-length and stress dependent variables, $P_r(i)$ is the probability of the crack being at a state *"r"* on the fracture surface after i cycles elapse and I_0 is the minimum number of cycles required for the crack to advance from one position on the fracture surface to the next and is also crack-length and stress dependent.

This derivation was made by defining the transition intensity λ_r and the Incubation time I_0 in the following form.

$$\lambda_r = \frac{B}{K} e^{Ki} \tag{2}$$

$$I_0 = C_3 [(r-1)^{n3} - r^{n3}] \tag{3}$$

where (4)

$$B = C_1 r^{n1} \tag{5}$$

$$K = C_2 r^{n2}$$

and C_1, C_2, C_3, n_1, n_2 and n_3 are material, applied stress and environment dependent parameters. These functions (eqs 2 and 3) were verified with the available crack growth scatter data based on the works of Virkler *et al.*[19] and Yang *et al.*[6].

As can be seen, identification of the six constants is sufficient to define eq. (1) at any crack position so as to calculate the associated number of cycles elapsed for any probability ($P_r(i)$) value. Carrying out this operation for a given probability value at all the crack states in a cumulative manner, will generate a crack-position versus number-of-cycles curve representing the probability with which a crack spends a certain number of cycles at any state.

Here, one should observe that the constants in these mathematical functions can be calculated by considering the crack growth curve obtained by using a continuum equation as being the $P_r(i) = 0.5$ curve. This can be done numerically, and the crack growth scatter at any crack length and at any fatigue load can be defined without the need to perform large number of fatigue tests. As mentioned before, the results of the model, when applied to A1 2024-T3 that was subjected to load cycles of constant amplitude, were in agreement with those experimentally obtained with the average error in the theoretical curves estimated to be 5%.

In order for the model to have a wider scope of application, it has to be substantiated for different loading conditions and for different materials. The first step in that direction is the verification of the model for different loading conditions on the same polycrystalline material. The experimental set-up and procedure used for this purpose are described in the next section.

DESCRIPTION OF THE EXPERIMENTAL SET-UP

Tests were conducted on Aluminium 7075–T6 alloy and crack-length versus number of cycles data were collected at three different stress levels. Each level was tested by using 60 identical specimens to establish the degree of crack-length scatter during propagation.

A rectangular specimen (320 mm × 101 mm) with a thickness of 3.175 mm and a center-cracked tension geometry was used throughout the test program. The direction of the center-crack chosen was perpendicular to the rolling direction of the sheet from which the specimens were cut as shown in Fig. 1. The dimensions of the specimen and the crack initiating notch are based on the ASTM E647 recommendations and are shown in Figs 2 and 3 respectively. The specimen ends were fixed to the test system by flat end grips whose dimensions are also based on the ASTM E647 recommendations.

A study was carried out to compare the available crack-length measuring techniques namely,

(a) The Photographic Technique,
(b) The Drop Potential Method,
(c) The Mechanical Method,
(d) The Electrical Technique,
(e) The Acoustic Method,
(f) The Ultrasonic Method and
(g) The Visual Method.

The results of this study, based on refs [20, 21 and 22] are detailed in ref. [23]. The conclusion was that the method of photographing the crack during propagation was the one most suited for the present program, since it is capable of tracing the growth of one point along the crack-front as opposed to a technique that measures the average position of the crack front.

The photographic technique used in this study depends on the reproduction of a sharp image of the deformed material along the flanks of the crack to make it possible to locate the crack-tip image and, consequently, to determine the crack-length with an acceptable degree of resolution. Since it is certain that in ductile materials, a sizable plastically deformed zone accompanies the crack during its propagation, especially in plane stress applications (see Fig. 4), this zone can be utilized as an accurate crack-length indicator. An example of this deformed zone is shown in Fig. 5. It can be seen that the interface between the two fracture surfaces (the crack) is not present along with this image. As the crack increases in length, leading to a higher crack opening displacement, the separation of the fracture surfaces becomes visible as a dark line within the deformed zone. This is shown in Fig. 6.

The testing configuration included a camera and a continuous light source positioned on one side of the specimen. The camera was triggered by an electrical pulse sent by a microcomputer that kept track of the elapsed number of cycles. Also, a number of shutter speeds, aperture settings, developing solutions, processing times and film types were experimented with to achieve the best

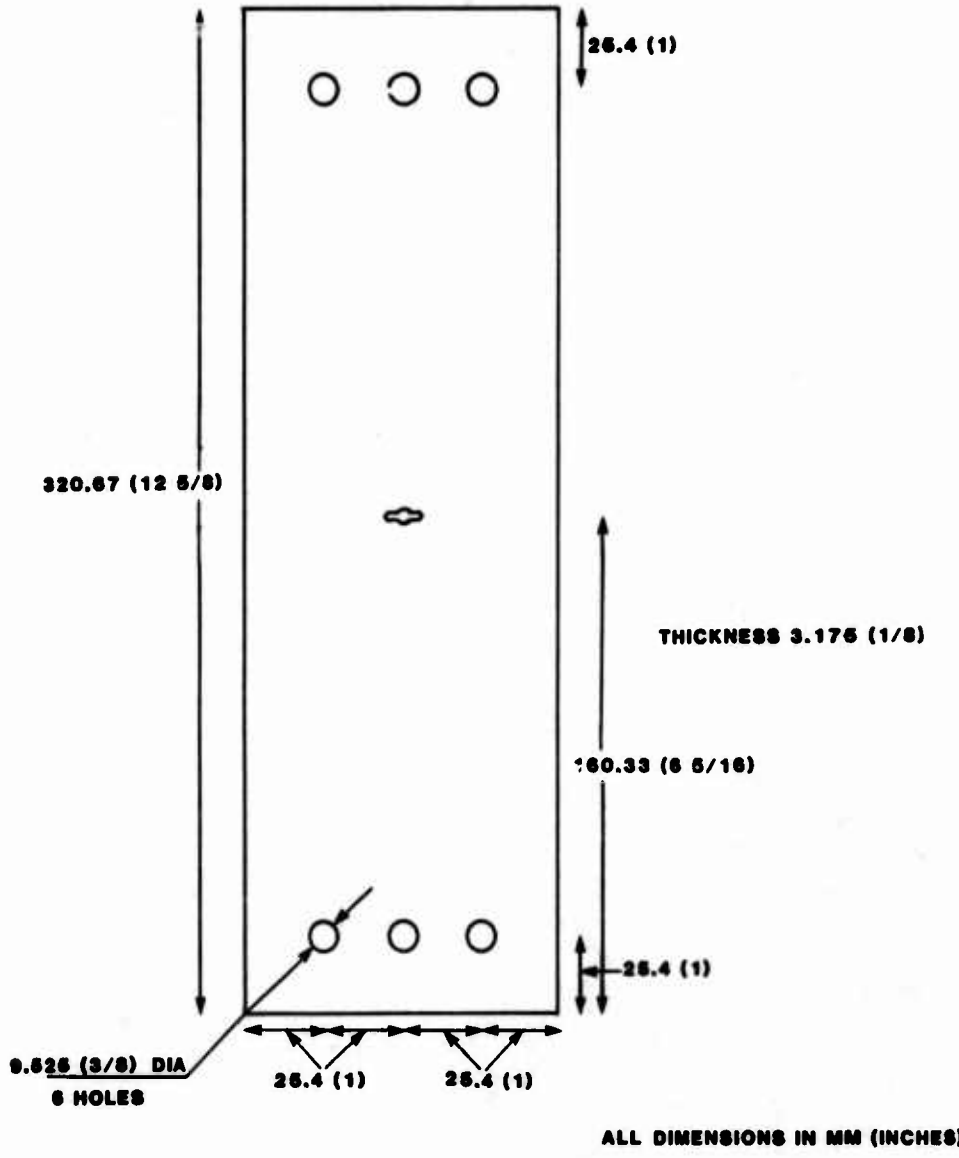

Fig. 2. Test specimen in the present study.

reproduction of this shear zone; these parameters are fully described in ref. [23].

A transmitted-light microscope equipped with a horizontal travelling table was used to determine the length of the image of the plastically deformed zone. The measurements were made by a digital micrometer having a resolution of 1 μm and transferred, after suitable interfacing, to a microcomputer for acquisition and subsequent analysis (see Fig. 7).

The error in these measurements was determined by comparing an actual crack-length, measured directly on the specimen's surface, and the length of its corresponding shear zone. This comparison, which was made in the cases of 1 × and 2 × magnifications (see in Table 1) indicated that the errors associated with the 2 × magnification, which was adopted throughout the test program, were lower. The region of interest used for recording the shear zone was limited to the central 28 mm on the 36 mm frame. Using a 2 × magnification, this meant that a maximum of 14 mm of crack growth was photographed in any test.

All the 180 tests carried out in this study were performed on a closed loop, servo-hydraulic Material Test System (MTS–880) capable of controlling loads within 0.2%.

Based on ASTM E647 recommendations, the initial crack-length, a_0 was chosen to be 10.00 mm; however, the crack-lengths were recorded from a length of 9.00 mm onwards. The final crack-length (a_f) for the purposes of this test program was limited to 23 mm measured from the center line of the test specimen. The loading parameters were then selected so that the crack transition from the normal mode to the shear mode could not occur before the crack reached this

specified length, i.e. 23 mm. This condition was imposed on the loading parameters in order to avoid the problem of defining the crack-length in the shear mode.

Tests were executed at three different stress ratios R; $R = P_{min}/P_{max}$, where P_{min} is the minimum load level and P_{max} is the maximum load level. The loading sequence for fatigue pre-cracking and the three test load conditions are detailed in Tables 2 and 3, respectively. A frequency of 10 Hz and a ramp waveform were selected for the loading cycle.

Figure 8 is an example of the results obtained in this test program showing the progress of the crack length at different loading cycles for one of the loading conditions.

EXPERIMENTAL RESULTS

As mentioned in the previous section sixty specimens were tested for three stress levels and crack-length (a) versus number-of-cycles (N); data was recorded from a length of 9 mm to a length of 23 mm. It may be recalled that the initial crack-length chosen for this test program was 10 mm and not 9 mm. Data between 9 mm and 10 mm will be used for future work on short crack. behaviour and the comparison between the theoretical probability crack-length versus number of cycles data. The experimental data will be made from the initial crack-length of 10 mm onwards. Crack-growth data (a vs N) for the three stress conditions is shown in Figs 9–11.

The next step in the analysis is the selection of the width-of-crack state for producing experimental data suitable for comparison with that generated by the mathematical model [15]. As can be seen from Table 1, the maximum error between the shear zone recorded on film and the crack-length measured from the specimen was estimated to be 0.163 mm. Using a conservative approach, the maximum error was assumed to be 0.2 mm and this was considered to be the state width.

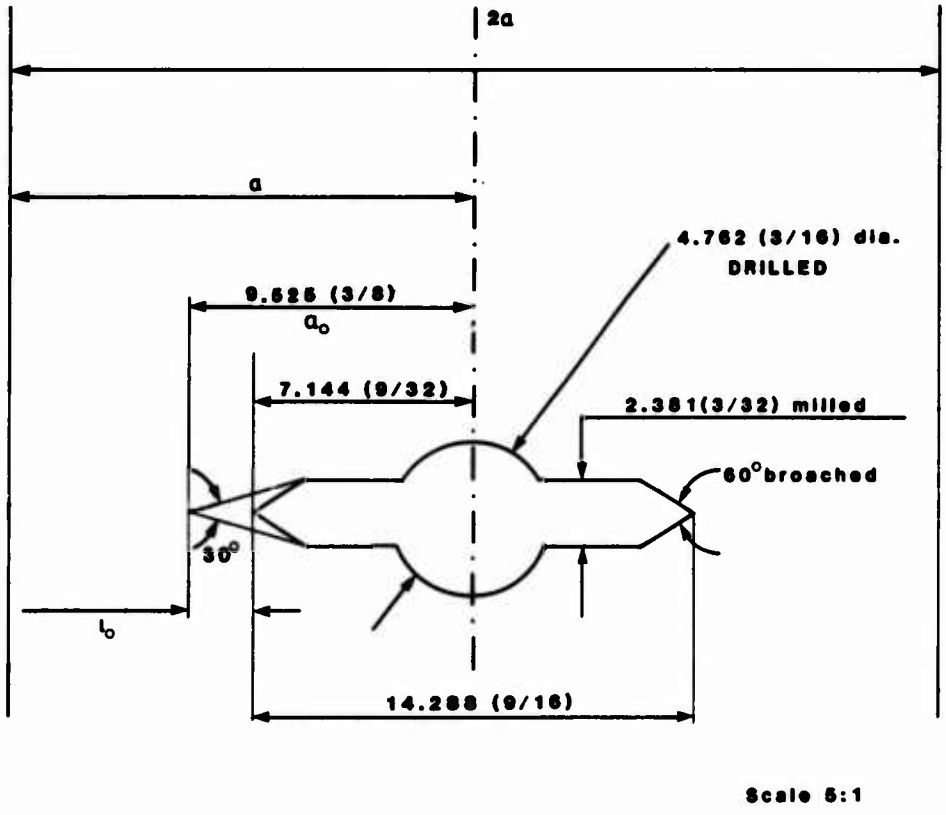

Fig. 3. Crack initiating notch.

Table 1. Comparison of the actual crack-length with the length measured from the film (all dimensions in mm)

Measured value (M)	Magnification (m)	Corrected (C) ($C = M/m$)	Actual (A)	Error ($A-C$)
4.882	1.058	4.612	4.831	0.218
8.047	1.045	7.700	7.755	0.055
11.624	1.045	11.123	11.206	0.083
18.855	1.045	18.043	18.082	0.039
8.208	2.000	4.104	4.202	0.098
17.028	2.000	8.514	8.677	0.163
15.950	2.000	7.975	8.042	0.067
17.692	2.000	8.846	8.924	0.078
19.841	2.000	9.920	9.956	0.035
23.023	2.000	11.501	11.592	0.090
26.161	2.000	13.080	13.153	0.072
29.803	2.000	14.901	15.018	0.116
31.623	2.000	15.811	15.892	0.081

Table 2. Loading sequence for fatigue pre-cracking (all loads in kN)

Test Condition	Load level till crack was generated (20 Hz)			Load level till crack reached 7.5mm (20 Hz)		
	P_{max}	P_{min}	ΔP	P_{max}	P_{min}	ΔP
I	25.95	8.30	17.65	26.55	13.55	13.00
II	29.30	7.70	21.60	24.80	10.65	14.15
III	26.30	7.70	18.60	21.50	7.30	14.20

Table 3. Test load conditions (all loads in kN)

Test Condition	Test load level (10 Hz)			
	P_{max}	P_{min}	ΔP	R
I	22.79	13.68	9.11	0.6
II	22.25	11.13	11.12	0.5
III	15.19	6.08	9.11	0.4

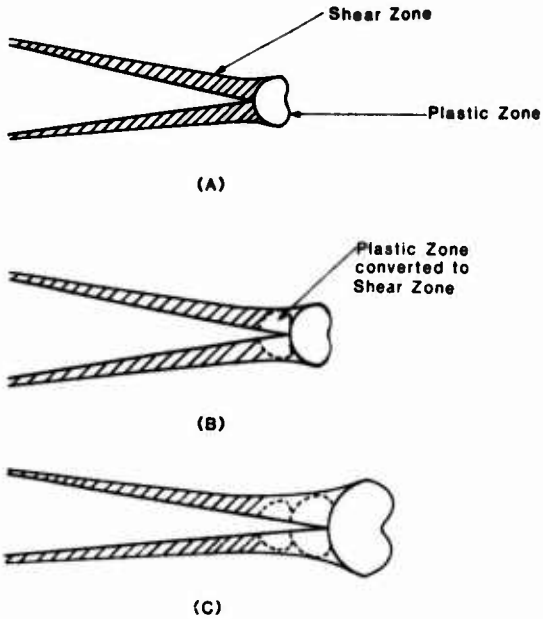

Fig. 4. Zone of plastic deformation in the vicinity of the fatigue crack[31].

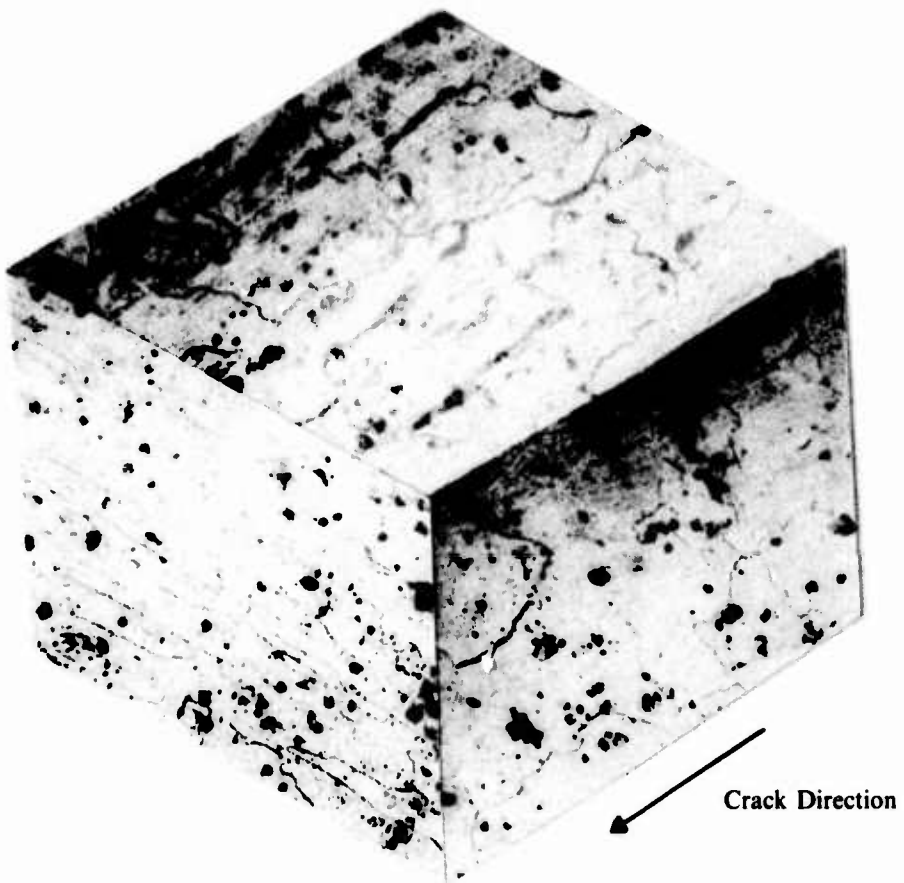

Fig. 1. Direction of crack with respect to the grain structure.

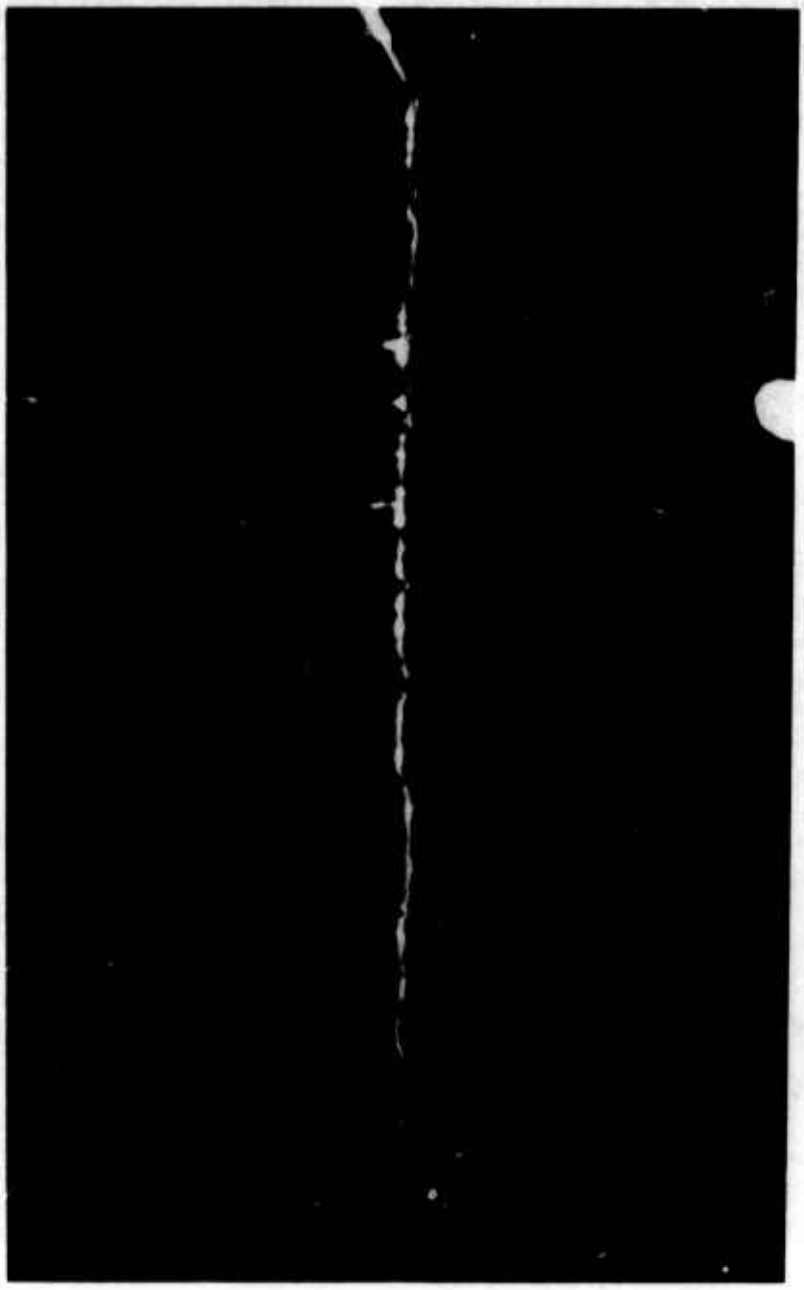

Fig. 5. Photograph of the shear zone accompanying the crack.

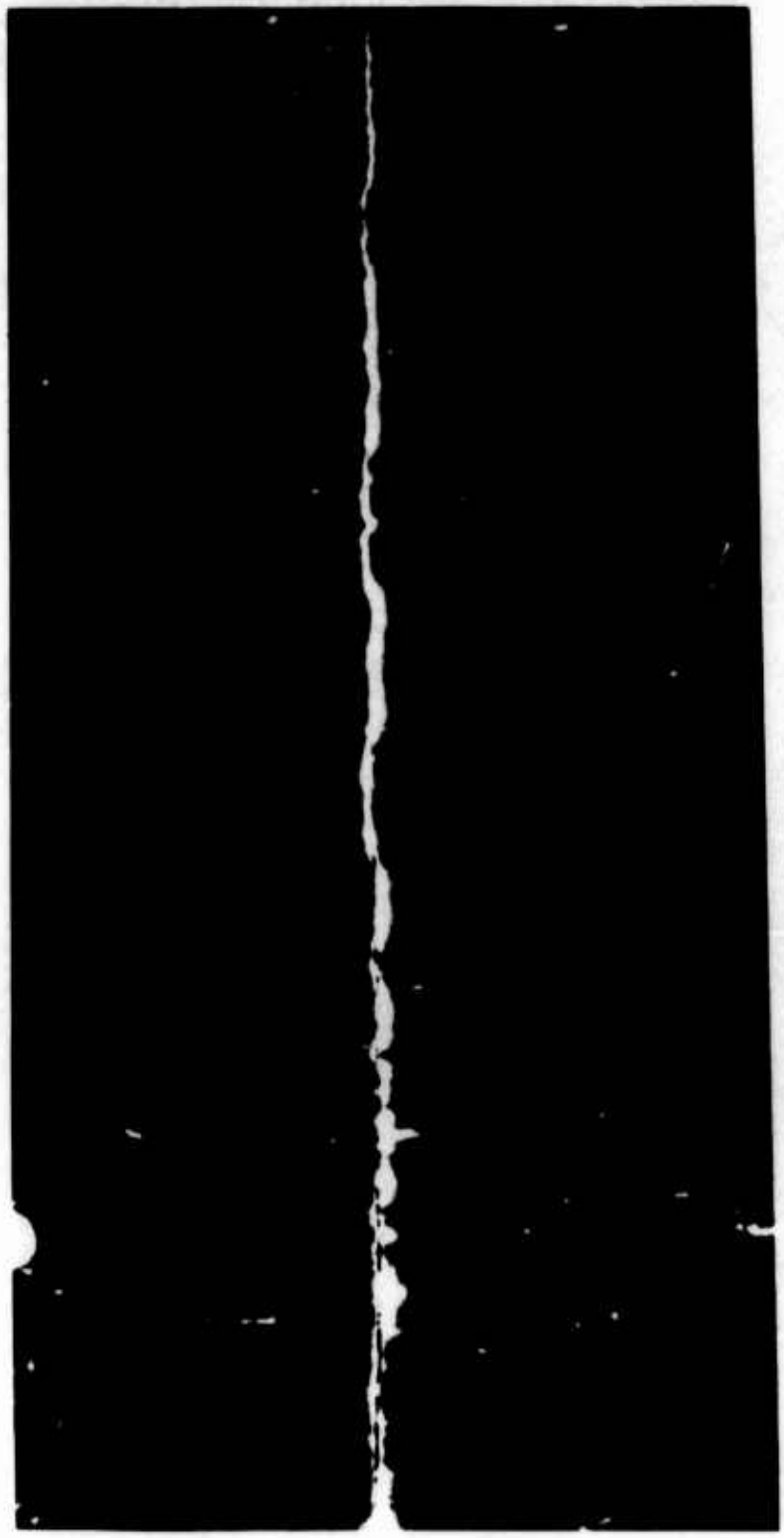

Fig. 6. Photograph of the shear zone with a visible separation of the crack surfaces.

1. Crack length = 9.495 mm
Number of cycles = 6380

2. Crack length = 10.498 mm
Number of cycles = 15510

3. Crack length = 10.912 mm
Number of cycles = 18960

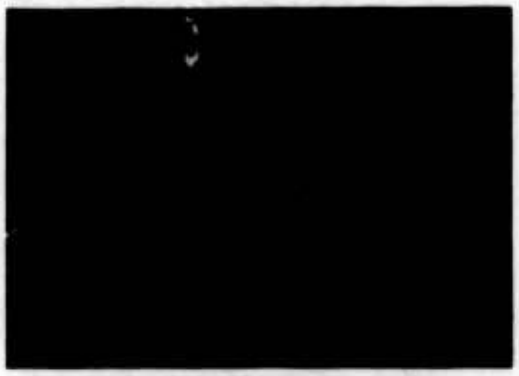

4. Crack length = 12.031 mm
Number of cycles = 25360

5. Crack length = 12.630 mm
Number of cycles = 28210

6. Crack length = 13.000 mm
Number of cycles = 29800

Fig. 8 Crack evolution as recorded from specimen number 1 subjected to Test Condition-II (Magnification 10X).

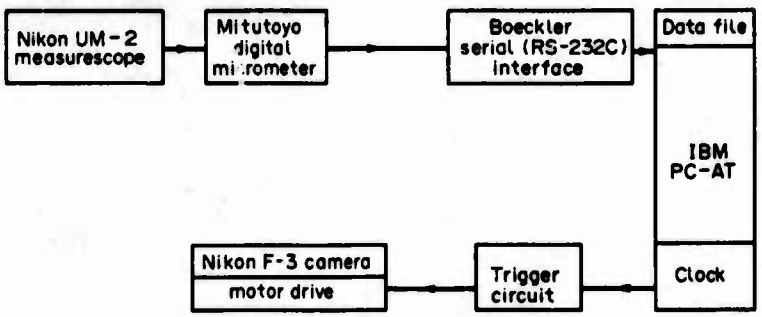

Fig. 7. Schematic of the camera-triggering and the crack-length measuring circuits.

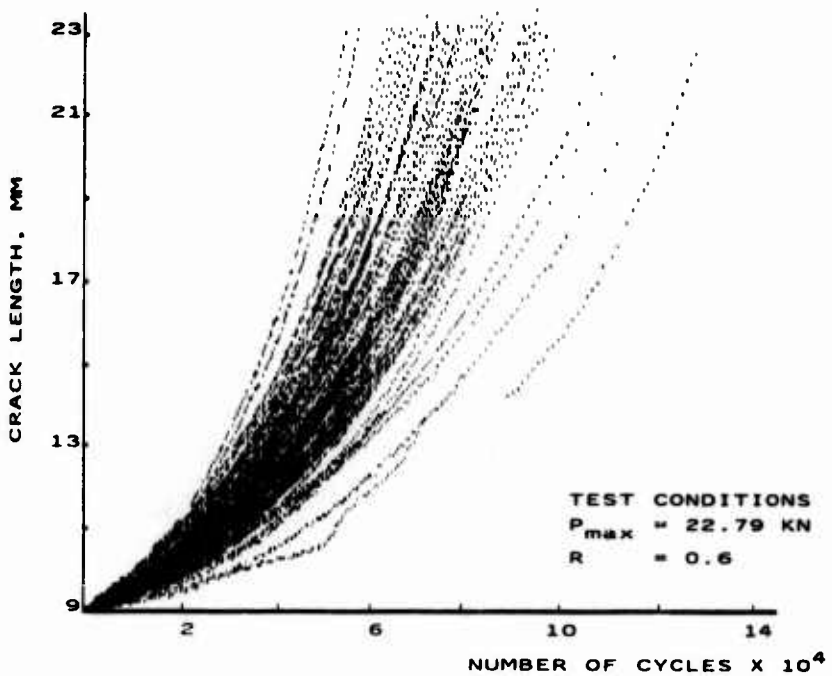

Fig. 9. Crack-length vs number of cycles data from 60 specimens for Test Condition I.

For a state width of 0.2 mm, the zone between 10 and 10.2 mm corresponded to an initial crack state (r_0) of 51 and the zone between 22.8 and 23 mm to a final crack state (r_f) of 115, leading to a total of 65 crack states. Similar to the approach discussed in ref. [15], the number of cycles spent by a crack in each of these 65 states was calculated by interpolation of the a vs N data. Thereupon, for all the stress levels, the interpolated values for each state in each of the sixty specimens was arranged in an ascending order. The lowest number of cycles was assigned a probability of:

$$P_r(i) = 1 - (x/60) \quad ; \quad x = 1$$

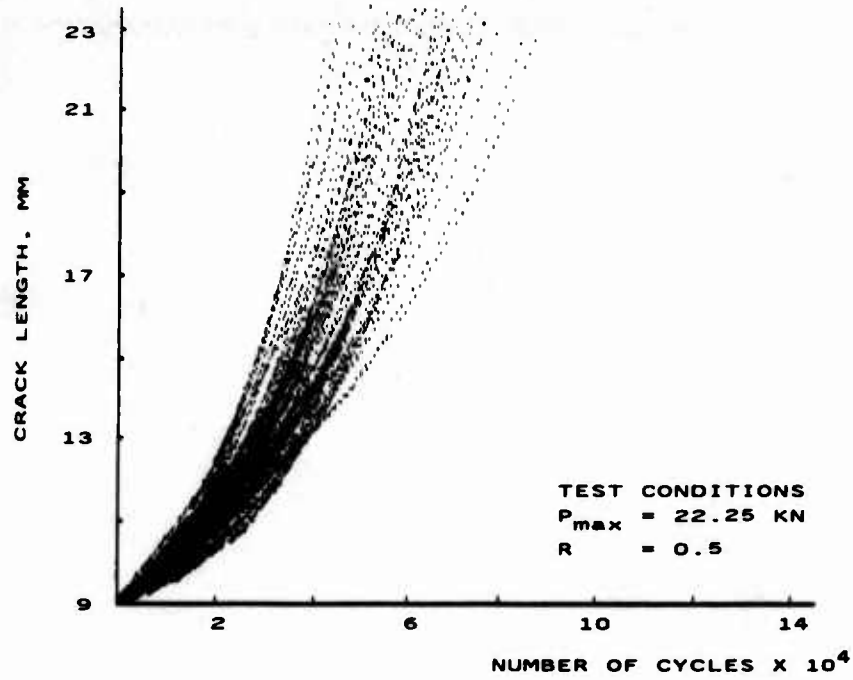

Fig. 10. Crack-length vs number of cycles data from 60 specimens for Test Condition II.

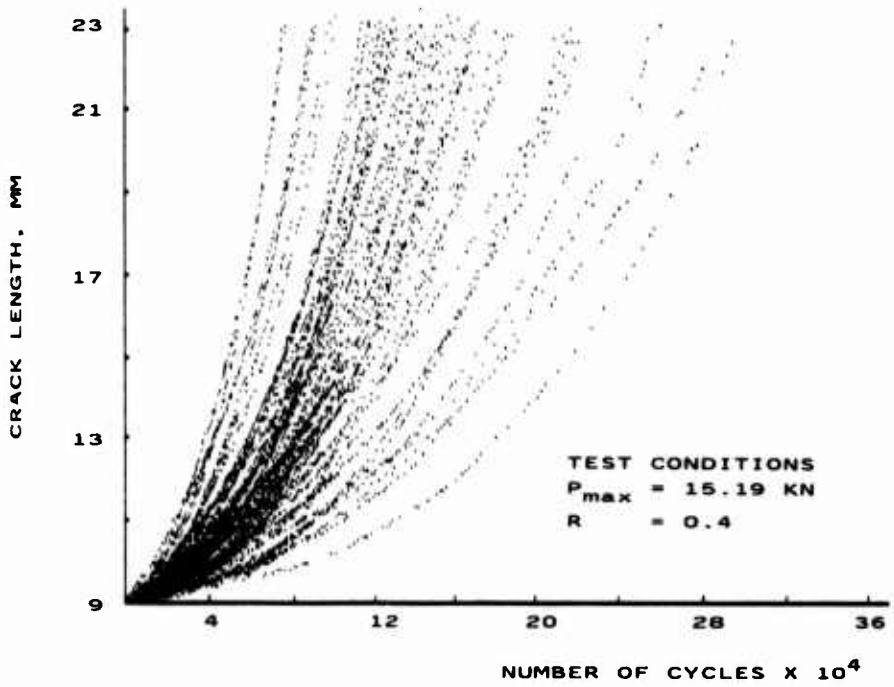

Fig. 11. Crack-length vs number of cycles data from 60 specimens for Test Condition III.

and so on up until the highest number of cycles whose corresponding probability value was:

$$P_r(i) = 1 - (x/60) \quad ; \quad x = 60.$$

A probability range of 0.9–0.1 was selected for comparison of the experimental and the theoretical data. The curves obtained experimentally are plotted in Figs 12–14 with the probability values having decrements of 0.1.

In these figures it is observed that the widest scatter band is associated with the test condition that produced the smallest mean crack-growth rate, Test Condition III, while the narrowest scatter band is associated with the Test Condition II in which the mean crack growth rate is the highest. This is due to the fact that when loads are high, the influence of the microstructure on crack propagation is diminished so that the degree of scatter of the a vs N sample curves, in relation to the mean growth curve, tends to be limited. Similar observations were made by Yang *et al.*[7] and this is perceptible in Fig. 15.

THEORETICAL RESULTS

Firstly, the continuum growth law to be utilized in the mathematical model was arrived at by investigating a number of crack growth equations with known material constants which recognize the effect of the stress ratio. Forman's equations[13,24] and the equation derived by Hardath *et al.*[25] fall into this category.

Forman's equation is generally written as:

$$\frac{da}{dN} = \frac{C(\Delta K)^n}{(1 - R)K_c - \Delta K} \tag{6}$$

where a is the crack-length, N is the number of cycles, K is the stress intensity factor range, K_c is the critical stress intensity factor, R is the stress ratio and C and n are material constants.

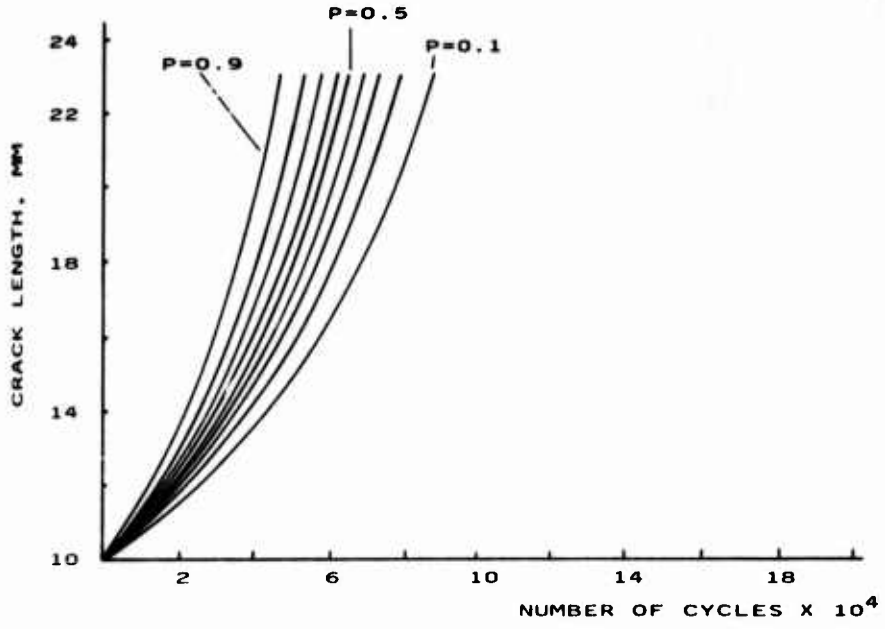

Fig. 12. Experimental constant-probability crack growth curves generated for Test Condition I.

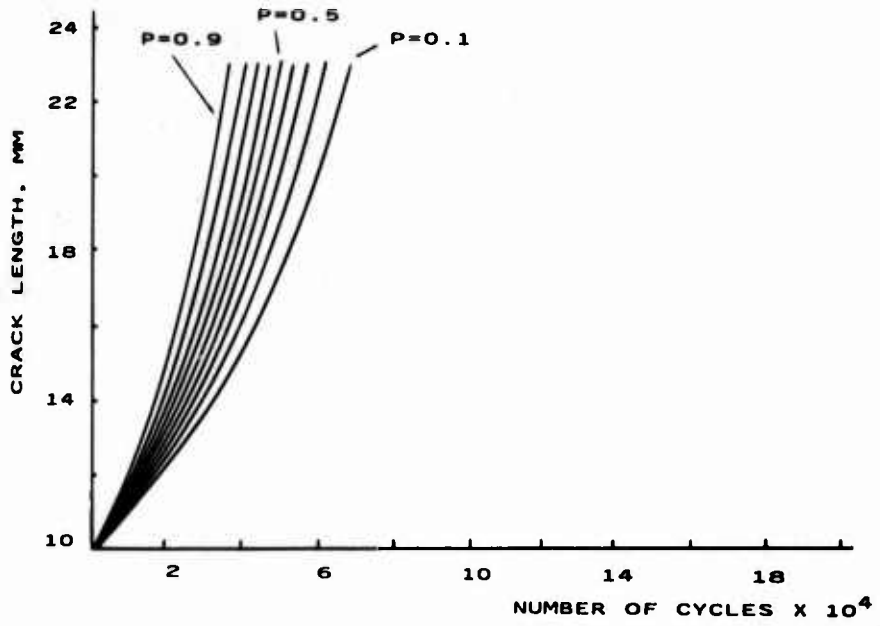

Fig. 13. Experimental constant-probability crack growth curves generated for Test Condition II.

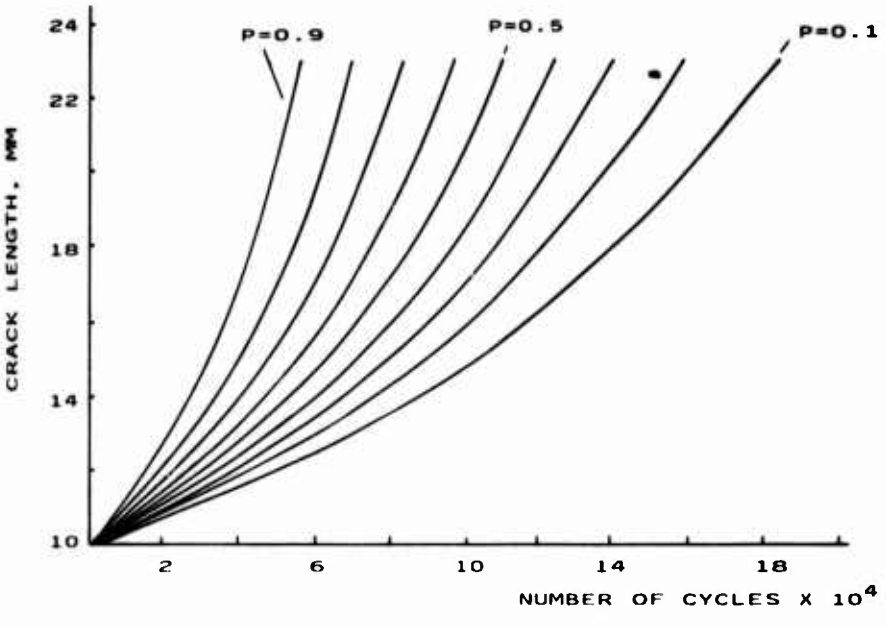

Fig. 14. Experimental constant-probability crack growth curves generated for Test Condition III.

The values of K_c, C and n for Aluminium 7075–T6 are listed in ref.[13] as:

$$K_C = 68 \text{ Ksi-in}^{\frac{1}{2}} (74 \text{ M Pa-}m^{\frac{1}{2}})$$

$$C = 5 \times 10^{-13} \text{ U.S. Customary Units}$$

$$= 1.63 \times 10^{-17} \text{ SI Units}$$

$$n = 3$$

and in ref.[24] as:

$$K_C = 40 \text{ Ksi-in}^{\frac{1}{2}} (44 \text{ MPa-}m^{\frac{1}{2}})$$

$$C = 2.13 \times 10^{-13} \text{ U.S. Customary Units}$$

$$= 1.60 \times 10^{-18} \text{ SI Units}$$

$$n = 3.21.$$

The equation derived by Hardarth *et al.*[25] is:

$$\frac{da}{dN} = C(\Delta \bar{K})^n \tag{7}$$

where
$$\bar{K} = \frac{K_{\text{eff}}}{\left(1 - \frac{K_{\max}}{K_f}\right)^2} \tag{8}$$

and
$$K_{\text{eff}} = (s_{\max} - s_0)\sqrt{\pi a}\, F \tag{9}$$

$s_{\max}$ is the maximum stress, s_0 is the crack opening stress, $\sqrt{\pi a}\, F$ is the stress intensity parameter for specimen configuration, $K_{\max}$ is the maximum stress intensity factor, K_F is the fracture parameter [81 Ksi-in$^{\frac{1}{2}}$ (89 M Pa-$m^{\frac{1}{2}}$)], C and n are material parameters.

$$C = 3.83 \times 10^{-8} \text{ SI Units}$$

$$n = 3.17.$$

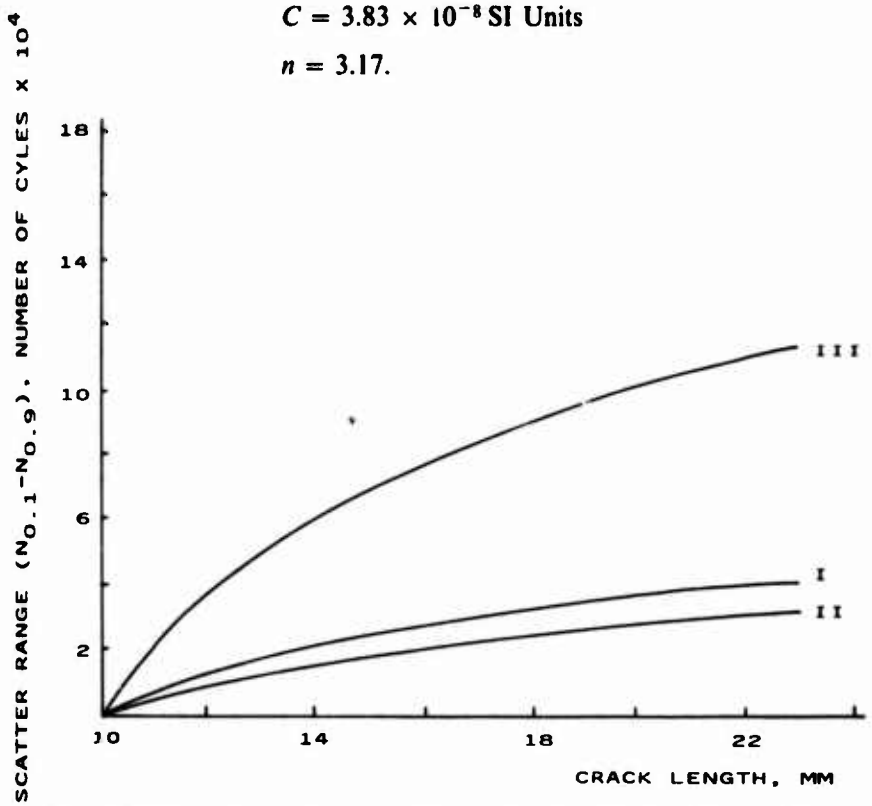

Fig. 15. Variation of the scatter range with crack length for the three Test Conditions.

Of the above two laws, the one provided by Forman *et al.*[13] was selected because it is based on data obtained from different laboratories as opposed to the equation of Hudson *et al.*[24] that was derived after correlation with one set of experimental data. The growth law of Hardarth *et al.*[25] was also not utilized because the present mean experimental growth rate was different from that predicted by the law, by an order of magnitude for all the three stress levels.

Having defined the continuum growth law and the corresponding material constants, the six constants C_1, C_2, C_3, n_1, n_2, n_3 were next calculated by obtaining their converged values using Newton–Raphson's method.

The six constants for each load condition are:

	I	II	III
C_1	0.015127	0.010064	0.010105
C_2	1.9371×10^{-6}	3.4055×10^{-6}	1.9758×10^{-6}
C_3	1.5940×10^{6}	1.0888×10^{6}	2.3151×10^{6}
n_1	0.8000	0.7957	0.8514
n_2	1.4946	1.4991	1.3501
n_3	−0.7000	−0.6820	−0.8537

Following the analysis presented in ref. [15] the theoretical probability curves were plotted making use of these constants, in Figs 16–18.

The percentage error of the number of cycles is plotted in Figs 19–21. The average value off the absolute errors was found to be 7%, 5% and 8% for the ', II and the III load conditions, respectively.

A remark is warranted on the six constants that characterize the crack growth scatter. Though these constants depend on the load parameters, no attempt has been made to derive an explicit relationship. In fact, there is no need for an explicit relationship since they are computed directly from the continuum growth law.

CONCLUSIONS

(1) The mathematical model developed here provides a physical description for fatigue crack propagation as well as capability of predicting crack growth scatter at different stress levels. While the model uses the crack growth data from a continuum law as its input, it does not depend on a specific law. The only requirement is that such a law must be a correct representation of the mean growth curve. The model has been validated for two aluminium alloys Al 2024–T3 and Al 7075–T6 subjected to four different stress levels and is in the process of being applied to steel and titanium alloys.

(2) The scatter data recorded for the second load condition ($\Delta P = 11.12$ kN, $P_{max} = 22.25$ kN) of the experimental program has been observed to be the least widespread when compared with that obtained from other load conditions with lower values of ΔP. This can be attributed to the following phenomenon. The crack transition from a specific state is governed by a critical threshold energy at the crack tip. When such a threshold is satisfied in one cycle or an accumulation of several cycles, depending on the load condition and crack-geometry, the crack tip can then advance from its present state to the following one. Hence for larger loads and longer crack-lengths, the probability that this propagation threshold is satisfied increases rapidly with the number of elapsed load cycles while, for smaller loads and shorter crack-lengths, the probability of discrete crack growth advancement increases gradually. In this hypothesis the degree of scatter in achieving the required threshold energy reflects on the degree of scatter of crack growth. Fractographic analysis of fracture surfaces shows that, at the same crack-length, more striations per unit distance are present along the fracture surface of specimens subjected to a large load level (Test Condition II, see Fig. 22b) than in the specimens subjected to a lower load level (the Test Conditions I and III, see Figs 22a and 22c). It is known that ductile fracture striations are formed due to a change in the orientation

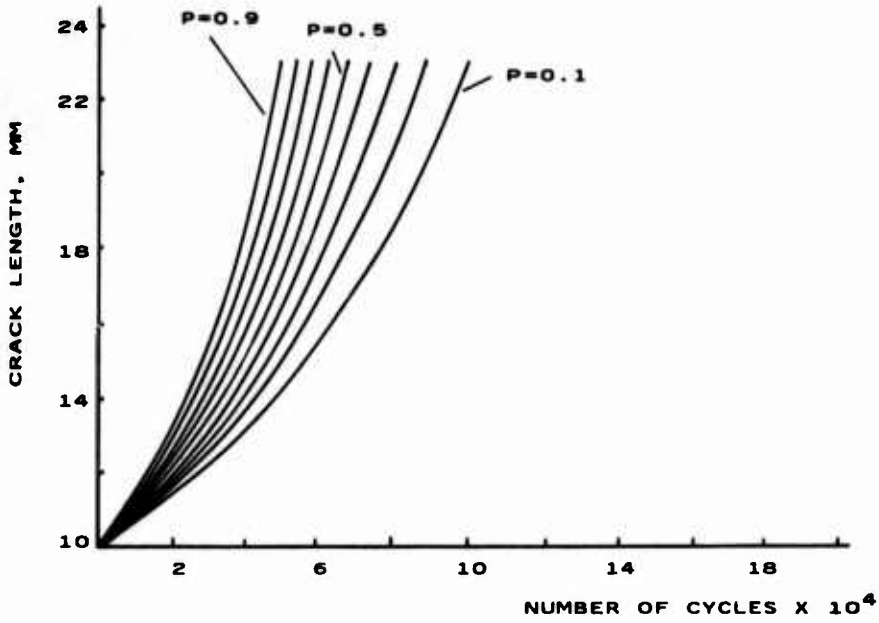

Fig. 16. Theoretical constant-probability crack growth curves generated for Test Condition I.

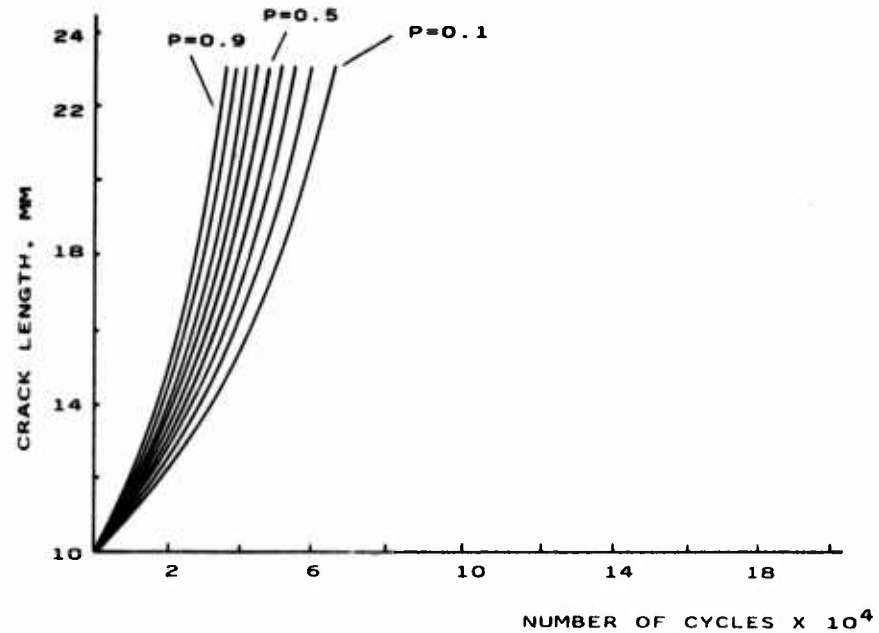

Fig. 17. Theoretical constant-probability crack growth curves generated for Test Condition II.

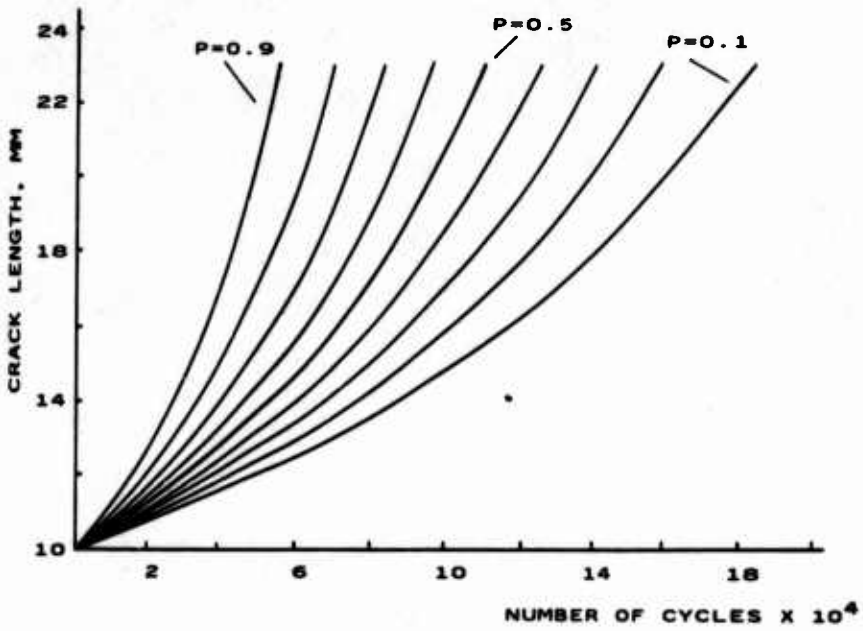

Fig. 18. Theoretical constant-probability crack growth curves generated for Test Condition III.

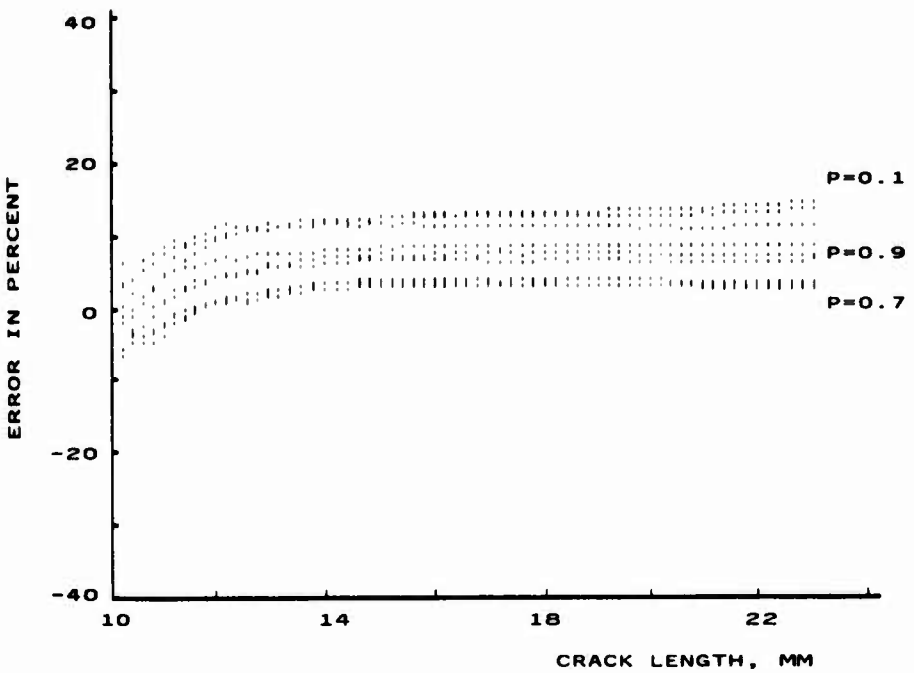

Fig. 19. Error in percent of the proposed model in the constant probability crack growth curves for Test Condition I.

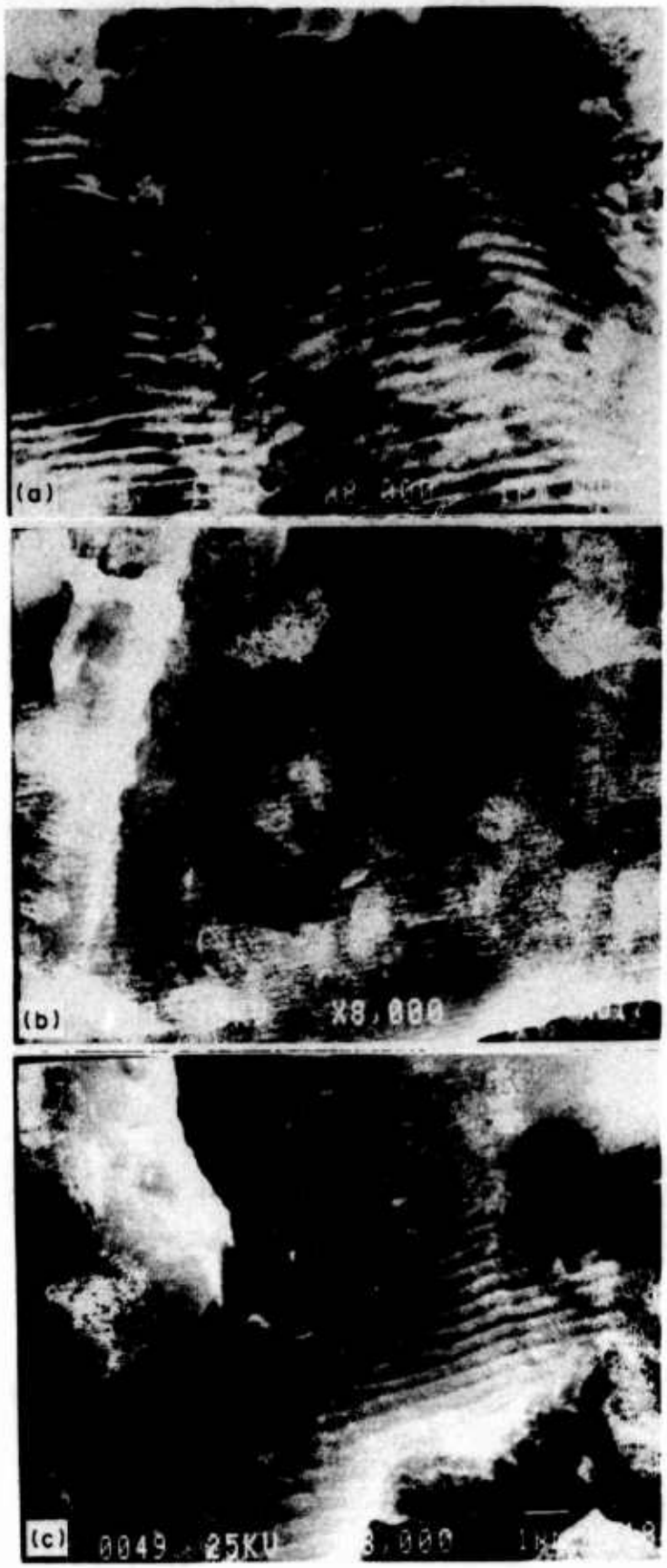

Fig. 22. (a) — (c)

Fig. 24. (a) — (b)

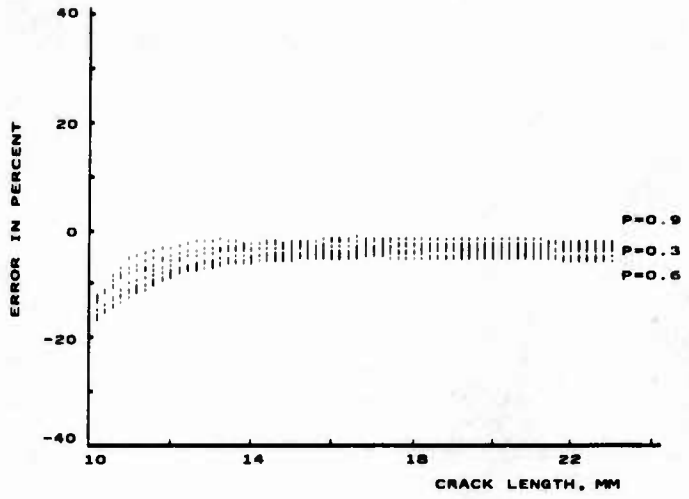

Fig. 20. Error in percent of the proposed model in the constant probability crack growth curves for Test Condition II.

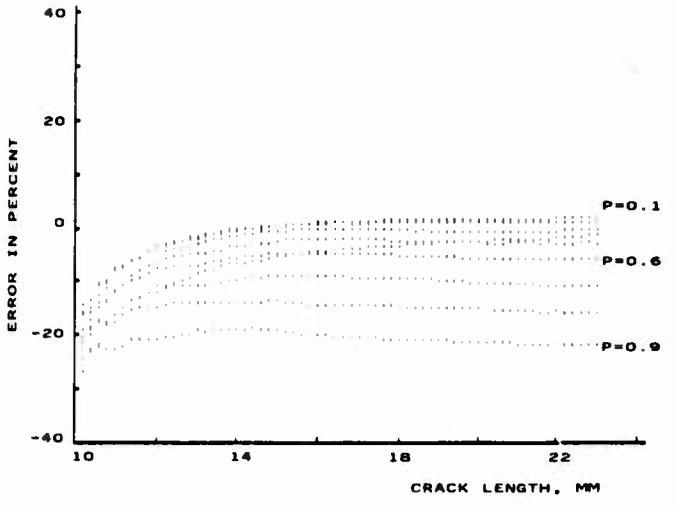

Fig. 21. Error in percent of the proposed model in the constant probability crack growth curves for Test Condition III.

of the fracture surface along a specific slip plane[26, 27]. Therefore, a denser striation pattern is observed at loading conditions associated with higher growth rates because numerous orientation changes take place in a unit distance of the fracture surface. It follows that the energy required for these changes is achieved more frequently under these conditions. Using this analogy at a macroscopic level, it can be said that the crack tip propagation threshold is also achieved more often. These observations may act as another factor that substantiate the fact that larger loading conditions result in a smaller degree of crack-growth scatter.

The changes in the orientation of the fracture surface along a specific slip-plane are reflected as the waviness of the crack path on the specimen surface. This is shown in Figs 23(a) and (b). In view of the explanation given previously, increased waviness of the crack path (measured in terms of the horizontal distance required for the crack propagation direction to change) is related to increase in the externally applied load levels and thus the degree of crack growth scatter at a particular load level could be related to the wavines of the crack path. Quantification of this dependence has not been attempted here.

The phenomenon of crack-tip branching was also observed. Typical examples are shown in Fig. 24(a) and (b). While the existence of branching certainly contributes to the degree of crack growth scatter due to random loss of propagation energy at the crack tip, the extent of this contribution is not known. Both the effect of the waviness and that of the crack-tip branching on the degree of crack growth scatter are under study by the authors.

(3) The use of the present model is directed towards two applications. The first is the constant amplitude loading which, while representing a simple load spectrum, does occur in practice; e.g. pressurization cycles in transport aircraft cabins, rotating bending stresses in generators, thermal stress cycles in pressure vessels. This application has been examined in this paper. The second application is the variable amplitude loading which could be a two-step load sequence (low-high, high-low) or a spectrum of random loads. Variable amplitude loading is, however, a complex problem due to the fact that the crack tip damage per cycle under such loading is not only controlled by the stress amplitude of the current cycle, but also by the preceding load history. It is generally agreed[28–30] that this dependence is only transient in nature and should not exist after a certain duration of cycling.

Reflecting this concept on the fundamentals of the constant-probability crack growth model, one observes two areas where modifications can be made to account for the history dependence of the crack growth process due to load changes. The first, is the assignment of appropriate mathematical functions for the variables B, K and I_0 to take this phenomenon into consideration. The Markovian approach in the model is not violated because even though the crack tip conditions depend on the loading history, the propagation process is affected only by the present crack tip conditions. On the basis of the existing works on variable amplitude loading, it can be said that the mathematical functions cannot be arrived at by simple superimposition. However, quantification of the crack growth rates for variable amplitudes, even in the deterministic sense has not been accomplished so far. Only if that is achieved, will modifications for B, K and I_0 be possible.

The other area where modification must be made is the consideration of initial crack-length (a_0). In the present model, a_0 was a constant as a result of an imposed experimental condition. Thus, the model provides a distribution of the number of cycles required for a crack to reach a specified discrete state from a_0. No attempt has been made to consider an initial crack-length distribution and the manner in which it will affect the constant probability curves. Attempts to interpret the constant-probability growth curves in terms of a distribution of crack states after a specified number of cycles have elapsed from the instant the crack reached a_0 were also not made. Only this type of a distribution is useful for variable-amplitude loading application because the history of the fracture process is described in terms of the number of cycles. The recognition of this distribution is an important step since it represents the initial crack-length configuration which is a necessary boundary condition for the new load spectrum.

Acknowledgement—This work was supported by the U.S. Air Force Office of Scientific Research under Contract AFOSR–85–0362 monitored by Dr. G. Haritos and Dr. N. Pagano.

REFERENCES

[1] D. W. Hoeppner and W. E. Krupp, Prediction of component life by application of fatigue crack growth knowledge. *Engng Fracture Mech.* **6**, 47–70 (1974).
[2] Karl-Heinz Schwalbe, Comparison of several fatigue crack propagation laws with experimental results. *Engng Fracture Mech.* **6**, 325–341 (1974).
[3] S. Chand and S. B. L. Garg, Propagation under constant amplitude loading, *Engng Fracture Mech.* **21**, 1–30 (1985).
[4] S. C. Saunders, On the probabilistic determination of scatter factors using Miner's rule in fatigue life studies. *ASTM STP* **511**.
[5] W. J. Plumbridge, Review: fatigue crack propagation in metallic and polymeric materials. *J. Mater. Sci.* **7** (1972).
[6] J. N. Yang, R. C. Donath and G. C. Salivar, Statistical fatigue crack propagation of IN 100 at elevated temperatures, *ASME Int. Conf. on Advances in Life Prediction Methods*, Albany, New York (1983).
[7] J. N. Yang and R. C. Donath, Statistics of crack growth of a super-alloy under sustained load. *J. Engng Mater. Technol.* **106**, 79–83 (1984).
[8] S. Tanaka, M. Ichikawa and S. Akita, Variability of m and C in fatigue crack propagation law $da/dN = C(\Delta K)^m$. *Int. J. Fracture* **17**, R 121–124 (1981).
[9] T. R. Gurney, *Fatigue of Welded Structures*, Cambridge University Press (1979).
[10] D. F. Ostergaard and B. M. Hillberry, Characteristic of the variability in fatigue crack propagation data, *Probabilistic Fracture Mechanics and Methods: Applications for structural design and maintenance*, *ASTM STP* **798**, 97–115 (1983).
[11] B. R. Ellingwood, Probabilistic Assessment of low cycle fatigue behaviour of structural welds, *J. Press. Vess. Technol.* 26–29 (February 1976).
[12] P. Paris and F. Erdogan, A critical analysis of crack propagation law, *J. bas. Engng* 528–534 (December 1963).
[13] R. G. Forman, V. E. Kearney and R. M. Engle, Numerical analysis of crack propagation in cyclic loaded structures, *J. Bas. Engng* 459–464 (September 1967).
[14] H. Ghonem and J. W. Provan, Micromechanics theory of fatigue crack initiation and propagation, *Engng Fracture Mech.* **13**, 963–977 (1980).
[15] H. Ghonem and S. Dore, Probabilistic description of fatigue crack propagation in polycrystalline solids. *Engng Fracture Mech.* **21**, 1151–1168 (1985).
[16] J. L. Bogdanoff and F. Kozin, *Probabilistic Models of Cumulative Damage*. John Wiley & Sons (1985).
[17] S. Aoki and M. Sakata, Statistical approach to delayed fracture of brittle materials, *Int. J. Fracture* **16**, 454–468 (1980).
[18] A. T. Bharucha-Reid, *Elements of the theory of Markov processes and its applications*. McGraw-Hill (1960).
[19] D. A. Virkler, B. M. Hillberry and P. K. Goel, The statistical nature of fatigue crack propagation, *J. Engng Mater. Technol.* **101**, 148–153 (1979).
[20] N. E. Frost, K. J. Marsh and L. P. Pook, *Metal fatigue*, Vol. 225. Clarendon Press, Oxford (1974).
[21] C. J. Beevers (Ed.), *Advances in Crack Length Measurement Techniques*. Chameleon Press, London, 1982.
[22] R. B. Thompson and D. O. Thompson, Ultrasonics in Nondestructive Evaluation. *Proc. IEEE*, 1716–1755 (December 1985).
[23] H. Ghonem and S. Dore, Probabilistic description of fatigue crack growth in aluminium alloys, AFOSR–83–0322, (April 1986).
[24] C. M. Hudson and J. T. Scardina, Effect of stress ratio on fatigue crack growth in 7075–T6 aluminium alloy sheet. *Engng Fracture Mech.* **1**, 429–446 (1969).
[25] H. F. Hardarth, J. C. Newman, Jr, W. Elber and C. C. Poe, Jr., Recent developments in analysis of crack propagation and fracture of practical materials, NASA TM–78766 (June 1978).
[26] R. W. Hertzberg and P. C. Paris, Application of electron fractography and fracture mechanics to fatigue crack propagation, *Proc. First Int. Conf. Fracture*, Sendai, Japan (1965).
[27] R. M. N. Pelloux and J. C. McMillan, Analysis of fracture surfaces by electron microscopy, *Proc. First Int. Conf. Fracture*, Sendai, Japan (1965).
[28] J. Schijve, Fatigue crack growth under spectrum loads, *ASTM STP* **595**, 3–23 (1976).
[29] W. Elber, Damage tolerance in aircraft structures, *ASTM STP* **486**, 230–242 (1971).
[30] R. Sunder, A mathematical model of fatigue crack propagation under variable amplitude loading, *Engng Fracture Mech.* **12**, 155–165 (1979).
[31] H. L. Ewalds and R. J. H. Wanhill, *Fracture Mechanics*, Vol. 176. Edward Arnold, London (1984).

(*Received* 29 *May* 1986)